

## 14. Flow Measurement Techniques in Turbomachinery

This chapter focuses on measurement techniques that have been used during experimental investigations of turbomachinery flow fields. These techniques are not fundamentally different from those used in other external flow studies. However, implementing them within turbomachines has introduced a series of unique and specialized issues in the preparation of the experimental setup, data acquisition, and analysis procedures. This chapter provides detailed information on the methods used to address these issues, along with a comprehensive summary on how they have been implemented to investigate complex flow phenomena within turbomachinery components.

<b>14.1 Background On Turbomachinery Flows ...</b>	<b>919</b>
<b>14.2 Non-Optical Measurement Techniques....</b>	<b>921</b>
14.2.1 Data-Acquisition Techniques .....	921
14.2.2 Non-Optical Measurement Techniques.....	928
<b>14.3 Optical Measurement Techniques .....</b>	<b>933</b>
14.3.1 Applications of Laser Doppler Velocimetry (LDV) ..	934
14.3.2 Applications of Particle Image Velocimetry (PIV) .	936
14.3.3 Applications of Laser Two-Focus Velocimetry (L2F) .....	945
14.3.4 Applications of Doppler Global Velocimetry (DGV)	948
14.3.5 Applications of Pressure-Sensitive Paint (PSP) ....	950
<b>14.4 Concluding Remarks .....</b>	<b>950</b>
<b>References .....</b>	<b>951</b>

### 14.1 Background On Turbomachinery Flows

Turbomachines constitute a large and diverse class of devices, which are used to transfer energy either to or from a flowing stream of fluid by the dynamic action of one or more moving blade rows. They have found a wide range of applications in many engineering systems such as:

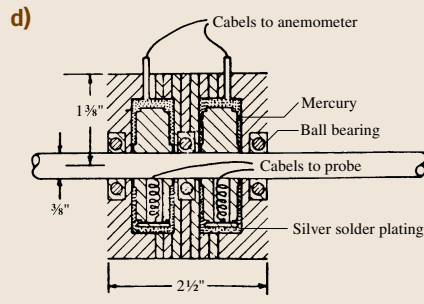
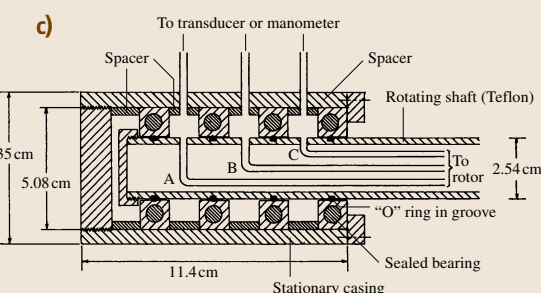
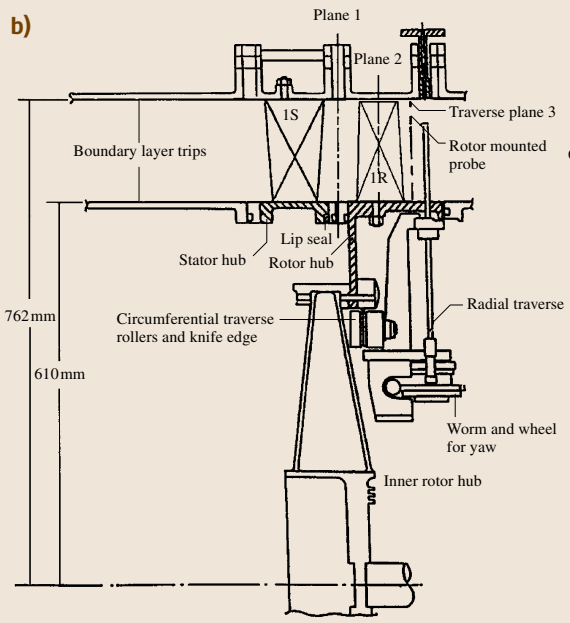
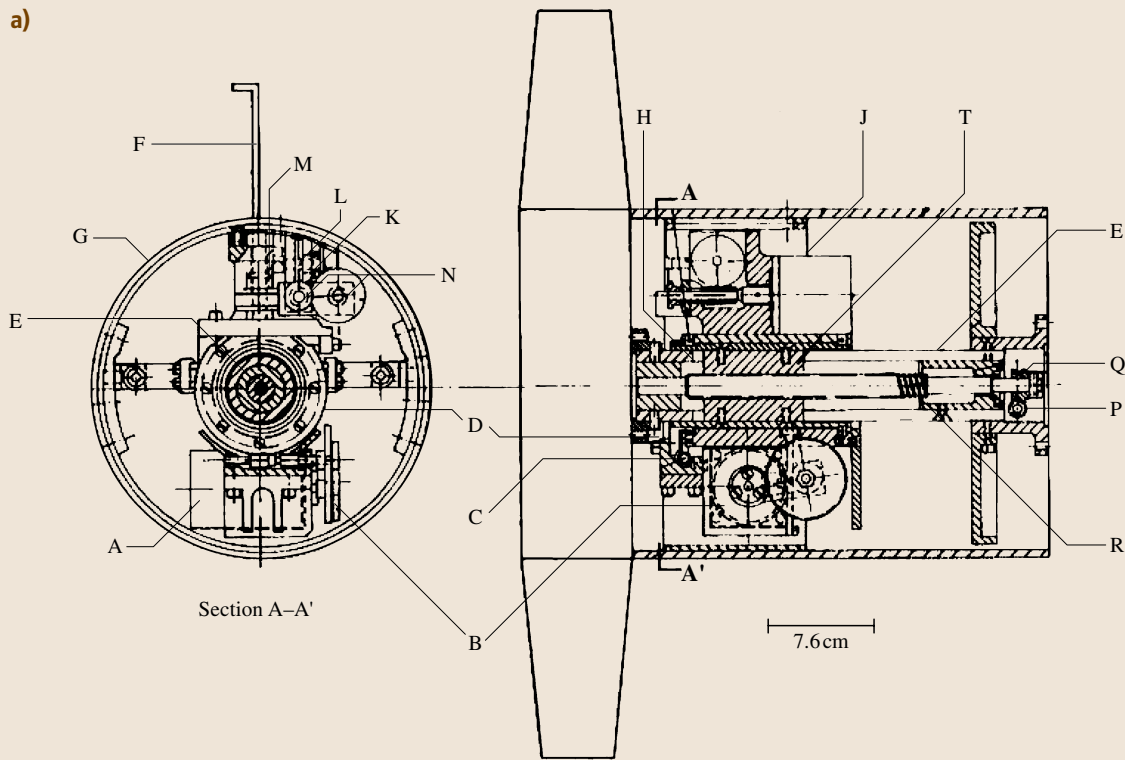
1. compressors and turbines in gas turbine engines used for power generation, propulsion of aircraft power, plants for naval surface ships, hydrofoil boats and hovercraft
2. propellers and rotors used in marine and aircraft propulsion
3. gas turbines and turbochargers used in land vehicles
4. steam turbines used in power plants
5. hydraulic turbines used in hydroelectric power plants
6. wind turbines
7. pumps used for transport of liquids, especially water, in a wide range of industrial, agricultural and residential applications
8. compressors used in industrial processes
9. pumps used in medical applications, e.g., in heart-assist devices

10. turbines and pumps used in liquid-fuel rocket engines

11. automotive torque converters, and many others.

Many books have already been published on the theory and applications of turbomachinery, and the reader should refer to them for guidance on design and analysis of components, and for information on associated fluid-mechanics and heat-transfer problems [14.1–8].

The complex flow fields within turbomachines are three-dimensional, turbulent, and inherently unsteady. Dominant unsteady phenomena occur due to the interactions of moving and stationary blades with nonuniform flow fields generated by upstream blades. For example, upstream wakes modulate the performance and modify the boundary layers on the blades, and in turn are chopped, strained, and the turbulence within them is modified as they pass through a rotor passage. Depending on applications, the boundary layers on blades range from the laminar to transitional and turbulent regimes. The associated flow fields are highly compressible within gas turbines, but often involve two phases



within pumps, inducers, hydroelectric turbines, and ship propellers. These complex flow phenomena affect the performance, efficiency, and range of operating conditions of these machines, as well as cause undesired phenomena, such as noise, vibrations, stall, and sometimes failure. Understanding of the flow dynamics and its effect on performance are essential for the development of more-efficient, reliable and quieter machines, as well as for developing physically meaningful and accurate prediction tools that can be incorporated into the design process. Such insight requires detailed experimental data on the mean and fluctuating components of the flow, pressure, and temperature, as well as on the resulting power, forces, torques, and vibrations. In this chapter we confine ourselves to flow and pressure measurements.

Numerous experimental studies have already investigated various aspects of the flow within turbomachinery over the years. These investigations have examined various three-dimensional, unsteady, and turbulent flow structures involving, e.g., blade–wake and wake–wake interactions, wake–boundary layer interactions, the

characteristics of curved rotor wake, the structure of turbulence and deterministic stresses, secondary flows, tip vortices and tip clearance flows, rotating stall and surge, shock waves and related unsteady phenomena, wake–shock interaction, rotor–stator clocking, mixing, cavitation, and many other topics. For measuring velocity and turbulence, these studies have used hot-wire/film anemometry, laser Doppler velocimetry (LDV), laser two-focus velocimetry (L2F) and particle image velocimetry (PIV). Pressure measurements have been performed using a variety of Pitot tubes including three-, four-, five-, and seven-hole probes, surface and probe-mounted pressure transducers, and pressure-sensitive paint (PSP), the latter for mapping the instantaneous pressure distribution over surfaces. This chapter summarizes the applications of these techniques and discusses issues that are specific to turbomachines. In addition to summaries, a series of tables provide examples of applications of the various measurement techniques. Each table is dedicated to a different class of sensors and contains a brief description of objectives and type of machine involved.

## 14.2 Non-Optical Measurement Techniques

This category includes a variety of probes, such as single or multisensor hot-wire/film anemometers; five-hole or other types of Pitot probes and high-frequency-response pressure transducers; measurements of static pressure, wall shear stress, and surface flow visualization on blade surfaces. Although not different from those used in other aero/hydrodynamic applications, their implementation in turbomachinery investigations introduces unique issues:

1. Acquisition of data in a rotating reference frame requires complex probe traverse mechanisms and data transmission systems.
2. The flow structure is inherently unsteady with contributions from periodic variations due to the relative alignment between rotor and stator blades, large-scale instabilities occurring below the de-

sign conditions such as stall and surge, as well as turbulence. Special data-acquisition and averaging procedures are needed to distinguish between these contributors in order to distinguish between them.

### 14.2.1 Data-Acquisition Techniques

#### Rotating Frame of Reference

Measurements in a rotating frame of reference require mechanisms for traversing probes in tangential, radial, axial, and *null* (probe aligned in the direction of the flow) directions. They also require means of data transmission from rotating to stationary frames, such as mercury or brush slip-ring units, pneumatic pressure-transfer devices, and wireless telemetry systems. In one of the earliest studies, *Weske* [14.11] measured pressure distributions on a rotor blade surface and traversed a Pitot probe across a rotor blade wake. He used a pulley-and-lever traverse mechanism as well as a selector switch and seal pressure-transmission system. *Gorton* and *Lakshminarayana* [14.12] used a three-sensor hot-wire to measure all three components of the mean velocity and turbulent stresses in a rotating frame of reference within a three-bladed rocket pump inducer

**Fig. 14.1a–d** Two sample rotating-frame traverse mechanisms: (a) *Lakshminarayana* [14.9] and (b) *Chaluvadi* et al. [14.10]; and examples of rotating-to-stationary frame data-transfer devices: (c) pneumatic pressure-transfer device, *Lakshminarayana* [14.9], and (d) mercury slip-ring unit, *Lakshminarayana* [14.9] ◀

**Table 14.1** Sample studies that have used hot-wire/film anemometry technique in investigating different aspects of turbomachinery flow fields. (S: stationary frame measurement, R: rotating frame measurement)

Hot-wire/film Author(s)	Year	Sensor type	Type of machine	Subject of study	Ref. frame
Lakshminarayana and Poncet [14.16]	1974	Hot-wire (X and single sensor)	Axial flow inducer	Rotor wakes	S
Gorton and Lakshminarayana [14.12]	1976	Hot-wire (three sensor)	Axial inducer	Mean flow and turbulence	R
Hah and Lakshminarayana [14.17]	1980	Hot-wire (three sensor)	Axial compressor	Effect of feestream turbulence on a rotor wake	S
Lakshminarayana et al. [14.18]	1982	Hot-wire (three sensor)	Axial fan	Effects of rotation and blade incidence on rotor wake	S
Dong and Cumpsty [14.19]	1990	Hot-wire (single and dual sensor)	Compressor cascade with upstream rods	Boundary layer	S
Hodson et al. [14.20]	1994	Hot-film (surface mounted)	Low pressure turbine	Unsteady boundary layer	S
Camp and Shin [14.21]	1995	Hot-wire, hot-film (single sensor)	Axial compressor	Turbulence intensity and length scale	S
Witkowski et al. [14.22]	1996	Hot-film (triple split)	Axial compressor	3-D wake decay and secondary flows	S
Halstead et al. [14.23]	1997	Hot-wire, hot-film (surface mounted), X hot-film probes	Axial compressor and turbine	Unsteady boundary layer	R and S
Hsu and Wo [14.24]	1997	Hot-wire (slanted)	Axial compressor	Unsteady wake	S
Sentker and Riess [14.25]	1998	Split hot-film	Axial compressor	Turbulence and unsteadiness	S
Ristic and Lakshminarayana [14.26]	1998	X Hot-wire	Axial turbine	3-D boundary layer	S
Prato et al. [14.27]	1998	Slanted hot-film	Axial compressor	Unsteady 3-D flow field	S
Furukawa et al. [14.28]	1998	Hot-wire	Diagonal flow rotor	Tip flow field	S
Sentker and Riess [14.29]	2000	Split hot-film	Axial compressor	Wake-blade interaction	S
Velarde-Suarez et al. [14.30]	2001	Hot-wire (dual sensor)	Centrifugal fan	Unsteady flow	S
Shin et al. [14.31]	2003	Hot-wire	Axial compressor	Blade boundary layers	S

passage operating in air. They did not have a rotating traverse system, and the probe was positioned manually while the inducer was not running. A rotating-probe traverse system, illustrated in Fig. 14.1a, was used by Reynolds et al. [14.13] to investigate the near wake of a rotor blade of an axial flow research fan. As described in detail in Lakshminarayana [14.9], this mechanism was mounted immediately downstream of the rotor, and allowed null and tangential traverse of a three-sensor hot-wire probe and a spherical head static pressure probe, while the rotor was in operation. Movements in the axial and radial directions could only be achieved manually, while the rotor was stationary. Dring and Joslyn [14.14] and Joslyn and Dring [14.15] reported measurements in the rotating frame of refer-

ence within an axial turbine facility. Their probes could be traversed along the tangential and radial directions while the machine was rotating. Recently, Chaluviadi et al. [14.10] used the rotating traverse mechanism shown in Fig. 14.1b, in a high-pressure turbine facility. This three-axis relative frame traverse mechanism had a computer-controlled stepper motor system, which allowed measurements within and at the exit of the rotor blade row.

To transmit and then measure pressure generated in the rotating frame to a stationary manometer or a transducer, early studies used pneumatic pressure-transfer devices, as shown in Fig. 14.1c [14.9]. The most common method to transmit data from embedded high-frequency pressure sensors or hot-wire signals has been

**Table 14.2** Sample studies that have used various types of Pitot pressure probes in investigating different aspects of turbomachinery flow fields. (S: stationary frame measurement, R: rotating frame measurement)

Pitot pressure probe					
Author(s)	Year	Sensor type	Type of machine	Subject of study	Ref. frame
Weske [14.11]	1947	Pitot probe, surface pressure	Axial rotor	rotor wake, surface pressure distribution	R
Neustein [14.38]	1964	Total pressure probes	Axial pump	Flow structure	S
Dring and Joslyn [14.14]	1981	Total pressure probes (Kiel)	Axial turbine	3-D flow structure	R
Joslyn and Dring [14.15]	1992	Five-hole probe, surface pressures	Axial turbine	3-D flow structure	R
Kang and Hirsch [14.39]	1993	Five-hole probe, flow viz.	Compressor cascade	Tip clearance effects	S
Carrotte et al. [14.40]	1995	Five-hole probe	Axial compressor	OGV flow field	S
Prato et al. [14.41]	1997	Five-hole probe	Axial compressor	Mean stator flow structure	S
Doukelis [14.42]	1998	Five-hole probe	Compressor cascade (annular)	Tip clearance effects	S
Ivey and Swoboda [14.43]	1998	Three-hole cobra probe, LDV	axial compressor	Tip leakage effects	R
Dey and Camci [14.44]	2000	Five-hole probe	Axial turbine	Tip clearance flow with coolant ejection	R
Xiao et al. [14.45]	2001	Five-hole probe, surface pressures	Axial turbine	Tip clearance flow and losses	R
McLean et al. [14.46, 47]	2001	Five-hole probe, Kiel probe	Axial turbine	Effects on coolant injection at upstream hub	R and S
McCarter et al. [14.48]	2001	Five-hole probe, LDV	Axial turbine	Tip clearance flow and losses	R
Coldrick et al. [14.49]	2003	Four-hole probe	Axial compressor	3-D flow structure	S
Pullan et al. [14.50]	2003	Five-hole probe	Axial turbine	Secondary flows	S
Gilarranz et al. [14.51]	2005	Five-hole probe	Centrifugal compressor	Flow structure	S

to use brush-type or mercury slip-rings. Figure 14.1d shows an earlier version of a two-channel mercury slip-ring [14.9]. Currently, a 150-channel brush-type system is being used at the axial flow turbine research facility (AFTRF) at the Pennsylvania State University [14.32]. Both brush and mercury slip rings are available commercially. Wireless telemetry systems also exist, but their implementation for unsteady pressure and velocity measurements has been rare, mostly due to their limited frequency response, which will most likely change in the future. Nevertheless, analog wireless telemetry was used in early measurements of rotor blade fluctuating and mean surface pressures [14.33, 34]. They also have been used to obtain temperature and strain data in real gas turbine engines [14.35–37]. A recently introduced digital wireless telemetry built for a high-pressure compressor rig [14.37] allowed simultaneous measurements in up to 48 channels with a bandwidth of 50 kHz. The analog version of this system supported 12 channels with a bandwidth of 30 kHz. The electrical power for

both systems was supplied using a contactless induction coil.

Recent examples of measurements in a rotating frame include investigations of the tip flow field of a turbine blade with coolant ejection [14.44]; of tip clearance effects in an axial flow turbine [14.45, 48] and in an axial flow compressor [14.43]; of blade-to-blade wake variability by *Boyd* and *Fleeter* [14.52]; and of blade row–wake and vortex interactions by *Chaluvadi* et al. [14.10], [14.53]. A more-comprehensive list of references is presented in Tables 14.1–14.4, where *R* in the last column indicates that the data have been acquired in the rotating frame of reference.

### Stationary Frame of Reference

Most of the experimental data have been obtained in a stationary frame of reference. Consequently, they require specialized phase-locked ensemble-averaging procedures during data analysis to distinguish between periodic and turbulent fluctuations [14.9, 16]. This ap-

**Table 14.3** Sample studies that have used high-frequency-response pressure sensors in investigating different aspects of turbomachinery flow fields. (S: stationary frame measurement, R: rotating frame measurement)

High-frequency response (HFR) pressure sensors					
Author(s)	Year	Sensor type	Type of machine	Subject of study	Ref. frame
Kerrebrock et al. [14.54]	1980	Spherical HFR-pressure probe	Axial compressor	Flow structure	S
Cousins et al. [14.55]	1981	HFR-pressure transducers (on rotors)	Axial compressor	Rotating stall	R
Giannissis et al. [14.56]	1989	HFR-pressure transducers	Axial compressor	Rotating stall	S
Cherrett and Bryce [14.57]	1992	HFR-pressure probe	Axial compressor	Rotor-rotor interactions, wakes and secondary flows	S
Ainsworth et al. [14.58]	1995	HFR-pressure probe	Axial turbine	Unsteady flow	S
Fabian and Jumper [14.59]	1995	HFR-pressure transducers (surface)	Axial compressor transonic cascade with upstream rods	Unsteady pressure distributions	S
Laborde et al. [14.60]	1997	HFR-pressure transducer on wall, flow viz.	Axial pump	Tip vortex cavitation	S
Dong et al. [14.61]	1998	HFR five-hole probe	Automotive torque converter	Unsteady flow	S
Roduner et al. [14.62]	1999	HFR-pressure probe	Centrifugal compressor	Impeller exit flow	S
Kost et al. [14.63]	2000	HFR-pressure sensor (surface)	Axial turbine	Unsteady flow	S
Mailach et al. [14.64]	2001	HFR-pressure transducer (surface)	Axial compressor	Rotating instabilities	R
Tiedemann and Kost [14.65]	2001	HFR-pressure probes , L2F	Axial turbine	Effect of clocking on wake-wake interactions	S
Lohrberg et al. [14.66]	2002	HFR-pressure transducers	Hydrofoil cascade	Cavitation	S
Nohmi et al. [14.67]	2003	HFR-pressure transducer (on wall and blade)	Centrifugal pump	Cavitation	R
Leger et al. [14.68]	2004	HFR-pressure sensor (flexible and on surface)	Axial compressor	Unsteady loading	S
Spakovszky [14.69]	2004	HFR-pressure transducer (on wall)	Centrifugal compressor	Rotating stall	S
Schleer et al. [14.70]	2004	HFR-pressure probe	Centrifugal compressor	Flow structure	S
Camci et al. [14.71]	2005	HFR-pressure probe	Axial turbine	Effect of tip geometry on tip leakage flows	

proach consists of conditionally sampling a time series of data obtained over many revolutions based on the phase or orientation of a rotor blade. A signal from a shaft encoder is typically used for synchronizing the sensor time series with the phase of the machine. For data recorded over  $N$  revolutions, the phase- or ensemble-averaged value of a certain flow variable  $\varphi$  at time or phase  $t_m$  in a revolution is

$$\bar{\varphi}(t_m) = \frac{1}{N} \sum_{n=1}^N \varphi_n(t_m) ,$$

where  $\varphi$  is the instantaneous value, e.g., of the velocity, pressure or temperature, and  $n$  an index indicating a certain period/cycle. The turbulent fluctuations are defined as the difference between the ensemble-averaged value and the instantaneous value

$$\varphi'_n(t_m) = \varphi_n(t_m) - \bar{\varphi}(t_m) .$$

If the number of samples per period is  $M$ , the time-averaged value is

$$\tilde{\varphi} = \frac{1}{M} \sum_{m=1}^m \bar{\varphi}(t_m) .$$



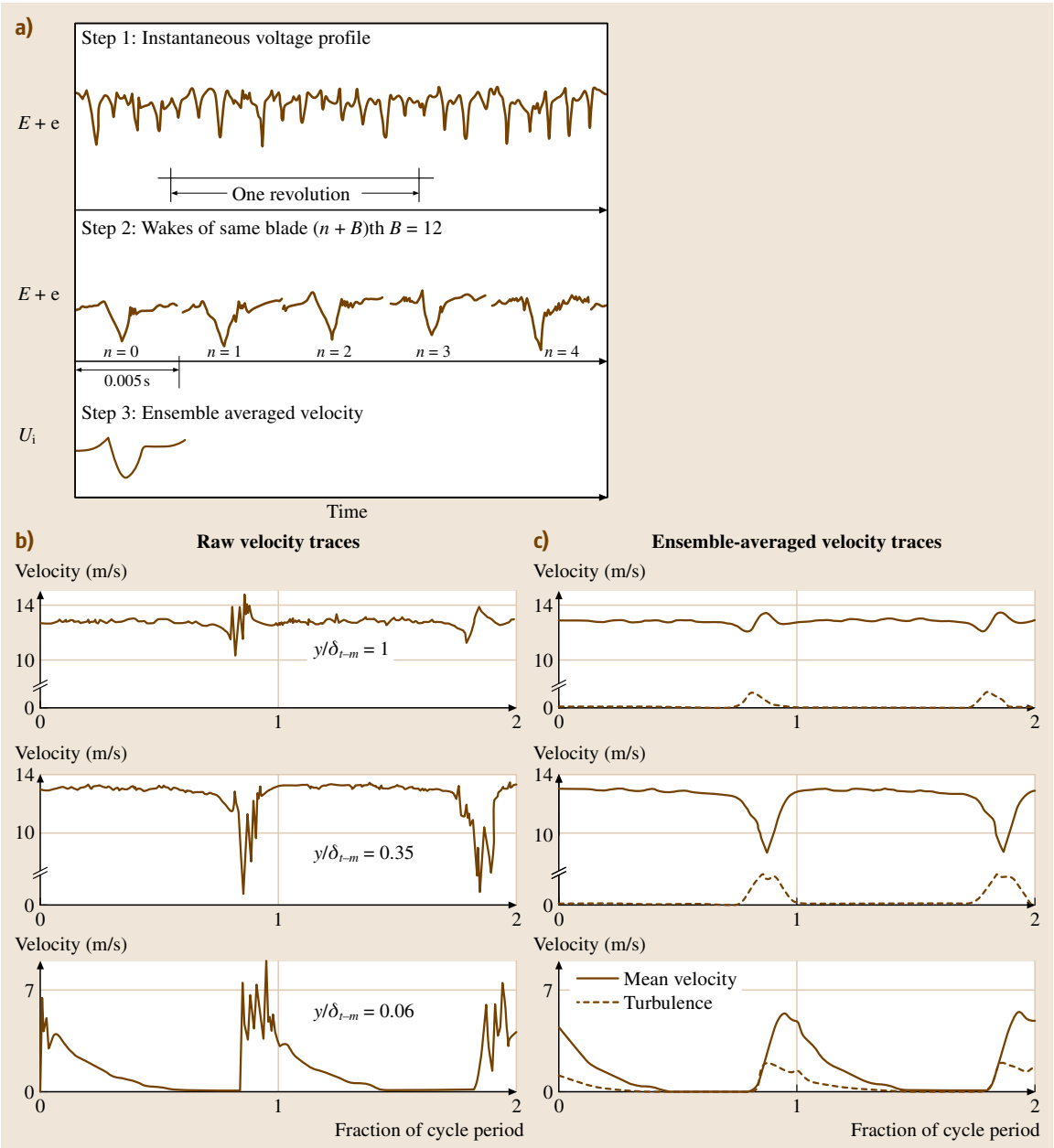
**Table 14.4** Sample studies that have used a combination of hot-wire/film anemometry, Pitot pressure probes and high-frequency-response pressure sensors in investigating different aspects of turbomachinery flow fields. (S: stationary frame measurement, R: rotating frame measurement)

Multiple sensors (hot-wire/film), Pitot and high-frequency pressure sensor					
Author(s)	Year	Sensor type	Type of machine	Subject of study	Ref. frame
Lockhart and Walker [14.72]	1974	Hot-wire (single sensor) pressure probe (three-hole Conrad-type yawmeter)	Axial compressor	Blade/wake interactions	S
Greitzer [14.73]	1976	Hot-wire, HFR-pressure probe	Axial compressor	Rotating stall and surge	S
Reynolds et al. [14.13]	1979	Hot-wire (three sensor), pressure probe (spherical head)	Axial fan	Rotor wakes	R and S
Gregory-Smith and Cleak [14.74]	1992	X hot-wire, five-hole probe	Axial turbine cascade	Secondary flows with inlet turbulence	S
Day [14.75]	1994	Hot-wire, HFR-pressure probe	Axial compressor	Rotating stall and surge	S
Kim and Fleeter [14.76]	1994	X hot-wire, HFR-pressure transducer	Axial compressor	Rotating stall and surge	R
Gallus et al. [14.77]	1994	Hot-wire, pressure probe (wake and blade surface)	Axial turbine	Secondary flows	R and S
Chaluvadi et al. [14.10]	2001	Hot-wire (three sensor), five-hole, three-hole and Kiel probes	Axial turbine	Blade–wake interaction	R and S
Reinmoller et al. [14.78]	2002	Hot-wire (three-sensor), five-hole probe	Axial turbine	Rotor–stator clocking	S
Sanders and Fleeter [14.79]	2002	X hot-film, HFR-pressure probe and surface transducers	Axial compressor	Blade–wake interaction and clocking	S
Johnston and Fleeter [14.80]	2002	Hot-film, HFR-pressure probe	Axial compressor	Wake–blade interaction	S
Boyd and Fleeter [14.52]	2003	Hot-wire, surface pressure (HFR)	Axial compressor	Blade-to-blade wake variability	R
Schoeiri et al. [14.81]	2003	Hot-wire (single), surface pressure	Low-pressure turbine cascade with upstream rods	Unsteady boundary layer	S
Chaluvadi et al. [14.53]	2004	Hot-wire (three sensor), five-hole probe	Axial steam turbine	Blade row–vortex interaction	R and S
Johnston and Fleeter [14.82]	2004	Hot-film, HFR-pressure probe	Axial fan	IGV-rotor potential field interaction	S

Figure 14.2a shows a sample signal from tri-axial hot-wire measurements, taken from *Lakshminarayana* [14.9], and illustrates the methodology described above to calculate the ensemble-averaged and the turbulence parameters using a continuous data time series. This approach has been widely used during analysis of hot-wire/film and pressure probe signals to study various aspects of the flow field behind rotating blade rows. Some sample references are listed in Tables 14.1–14.4, and a sample application is presented in Fig. 14.2b, showing the velocity traces obtained using a hot-wire

anemometer, within a compressor cascade operating downstream of a row of rotating cylindrical rods [14.19].

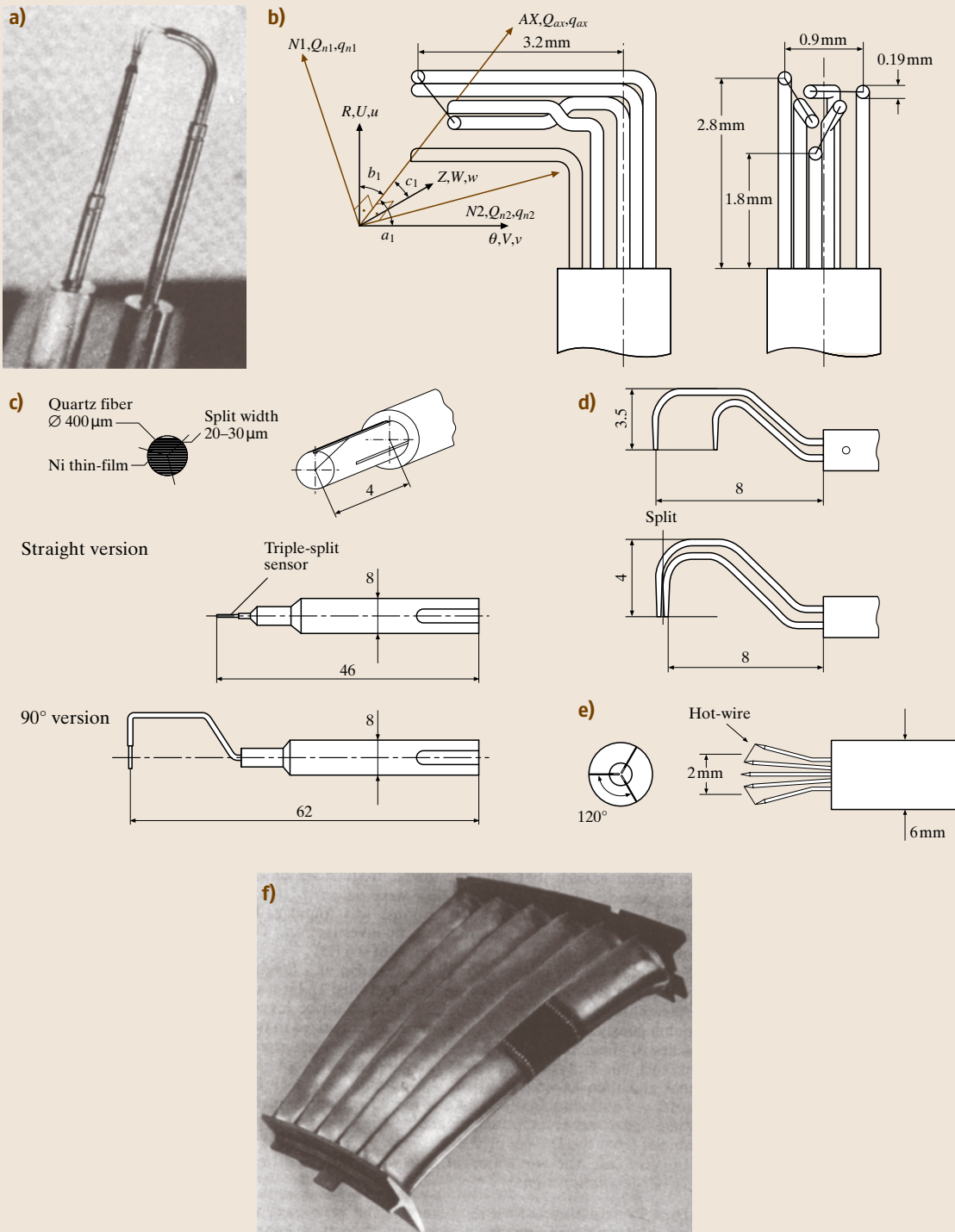
The so-called *phase-locked averaging technique* is another variation of the phase-dependent data acquisition and averaging methods. In this approach, the sensor is triggered based on a signal provided by the encoder to acquire data during a short but finite time  $\delta t$  at a fixed phase of the revolution. Different phases can be sampled by varying the delay between the shaft encoder pulse and timing of data acquisition. After collecting data over  $N$  cycles, the time delay is changed to obtain an average



**Fig. 14.2a–c** Stationary-frame data acquisition and reduction procedures for hot-wire signals. **(a)** The methodology to calculate the ensemble-averaged data from continuous instantaneous time series, as explained in Lakshminarayana [14.9]. **(b), (c)** A sample application of the same measurement methodology in a compressor cascade experiment with upstream rotating rods (after Dong and Cumpsty [14.19])

**Fig. 14.3a–f** Examples of various hot-wire/film probes used in turbomachinery flow investigations. **(a)** Lakshminarayana and Poncet [14.16], **(b)** Gorton and Lakshminarayana [14.12], **(c)** Witkowski et al. [14.22], **(d)** Sentker and Riess [14.25], **(e)** Chaluvadi et al. [14.53]. **(f)** Surface mounted hot-film Hodson et al. [14.20] ►





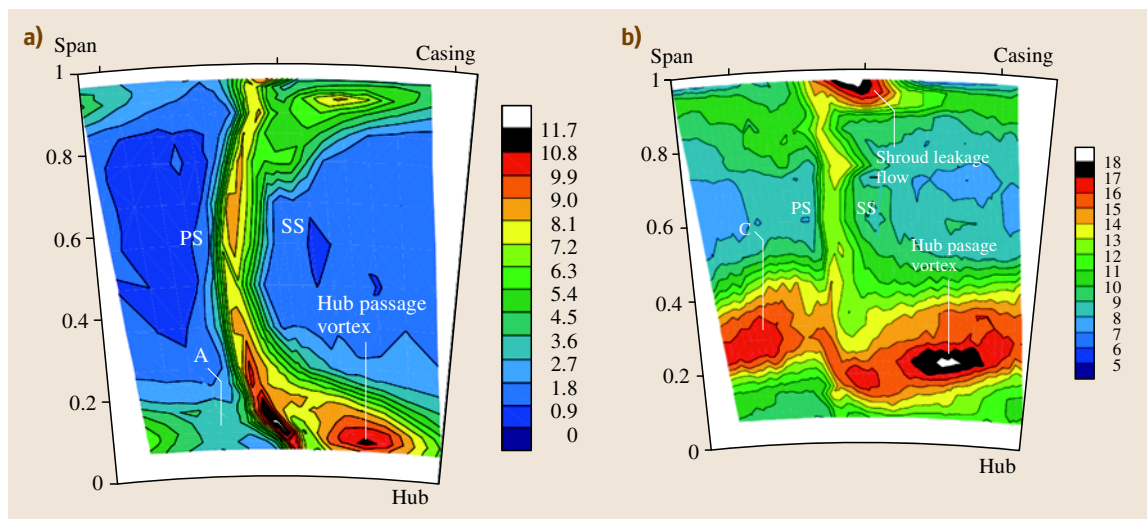


**Fig. 14.4a,b** Turbulence intensity contours measured using a three-sensor hot-wire behind (a) the stator and (b) the rotor of a high-pressure axial-flow steam turbine stage, with upstream delta wings used to simulate the rotor passage vortex (after Chaluvadi et al. [14.53])

at another phase of the rotor period. This procedure has not been used as extensively, and the reader is referred to Lakshminarayana [14.9] for background, and to Hsu and Wo [14.24] for an example of implementation.

Camp and Shin [14.21] used another approach to filter out the periodic components of a signal, i.e., those occurring at the blade-passing frequency. They used a Fourier transform to obtain the spectrum of a signal and zeroed the amplitude at the blade-passing frequency and its harmonics. The filtered Fourier transform was then transformed back into the time domain to obtain the turbulent signal. The modulated spectrum was also used for calculating the autocorrelation function directly from the Fourier coefficients, which provided the turbulent length scale. The authors claimed that these procedures were computationally efficient, and required a comparatively small amount of data. These advantages enabled them to measure the turbulence in a large number of points over a stator passage.

## 14.2.2 Non-Optical Measurement Techniques

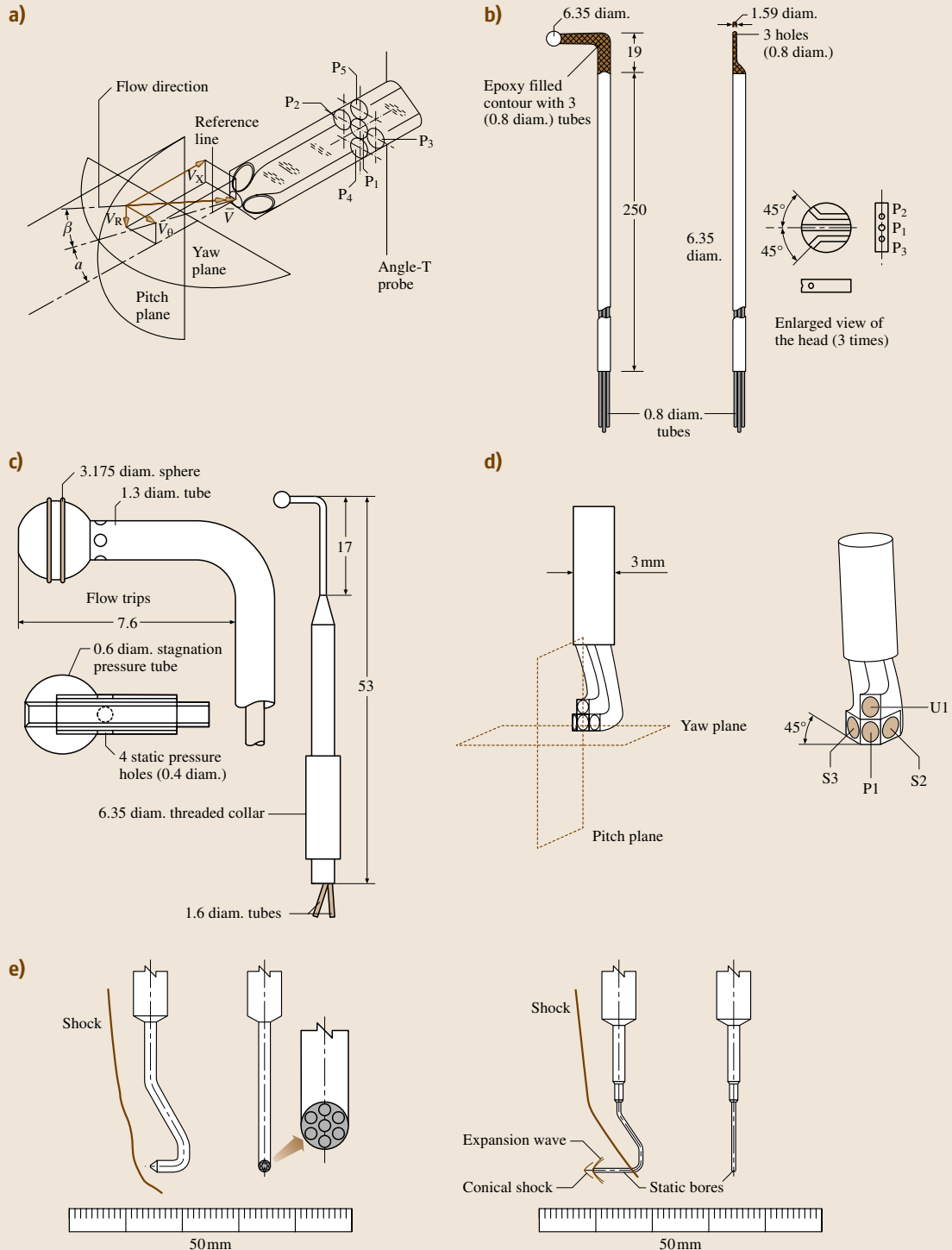
### Hot-Wire/Film Anemometry

Due to their small size and high-frequency response, hot-wire and hot-film anemometers have been used extensively in investigations of turbomachinery flow fields. Extensive background and technical information on these techniques can be found in Bruun [14.86], Gold-

stein [14.87] and other chapters in this book. A hot-wire probe consists of a short length ( $\approx 1$  mm), fine-diameter ( $5\text{ }\mu\text{m}$  or less) wire made of tungsten, platinum or platinum alloys, which is attached to two prongs. Hot-film sensors are thin (about  $0.1\text{ }\mu\text{m}$ ) platinum or nickel films deposited on thermally insulating substrates (usually quartz), which are typically shaped as cylinders, wedges or cones. For surface measurements, hot-film sensors can be glued to the wall. In cylindrical hot-film probes, the active element is usually  $25\text{--}70\text{ }\mu\text{m}$  in diameter and  $1\text{--}2$  mm long. Compared to hot-wire probes, the hot-film probes have a more-rigid construction, are less susceptible to contamination, and have more long-term calibration stability. Consequently, they have a lower frequency of breakage. However, it is more expensive to replace them, they have a more-complex frequency response, and their calibration may be affected by their own vortex shedding [14.86].

Early investigations in turbomachinery flows using hot-wire/film probes were mostly qualitative [14.72, 88, 89]. However, with the implementation of rotating-frame measurement techniques as well as the

**Fig. 14.5a–e** Sample Pitot pressure probes used in turbomachinery flow investigations: (a) five-hole probe Treaster and Yocum [14.83], (b) disk-type boundary-layer probe Sitaram et al. [14.84], (c) spherical head probe Sitaram et al. [14.84], (d) four-hole probe Coldrick et al. [14.49] and (e) seven-hole probe Gottlich et al. [14.85]►



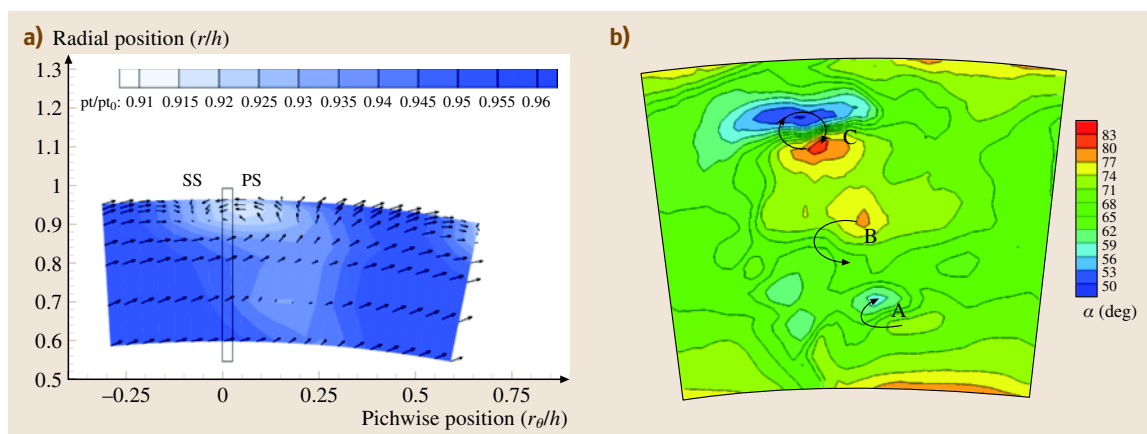


**Fig. 14.6a,b** Sample data obtained using five-hole probes. **(a)** Pressure-loss contours and velocity vectors downstream of an axial-flow turbine rotor. These measurements were performed in the rotating frame by Dey and Camci [14.44]. **(b)** Meridional yaw angle ( $\alpha$ ) contours at the exit of a nozzle guide vane, Pullan et al. [14.50]

stationary-frame acquisition and averaging methods, as described above, substantial amounts of quantitative experimental data have been collected on various aspects of the flow within turbomachines. Many different types of hot-wire and hot-film probes have been used, including single-, dual-, or triple-sensor hot-wire probes, single-element or double/triple split hot-film probes, as well as surface-mounted hot-film sensors for surface shear stress measurements. Characteristic examples of the types of probes used in investigating turbomachinery flows are presented in Fig. 14.3. Figure 14.4 shows sample turbulence intensity contours obtained within a high-pressure axial flow steam turbine stage, using the three-sensor hot-wire probe shown in Fig. 14.3e [14.53]. This specific test rig contained a stator row followed by a rotor row. This study investigated the impact of the upstream rotor passage vortex, which was simulated using delta-wing vortex generators located upstream of the stator row, on the performance of the downstream blade rows. Hot-wire measurements were performed in the stationary frame of reference and the ensemble-averaging technique was used to obtain the spatial distribution of turbulence intensity. Table 14.1 provides samples of other applications of hot-wire/hot-film anemometry, showing the types of probe and machine as well as the main topic of investigation. Studies involving hot-wire/hot-film measurements along with other sensors are summarized in Table 14.4.

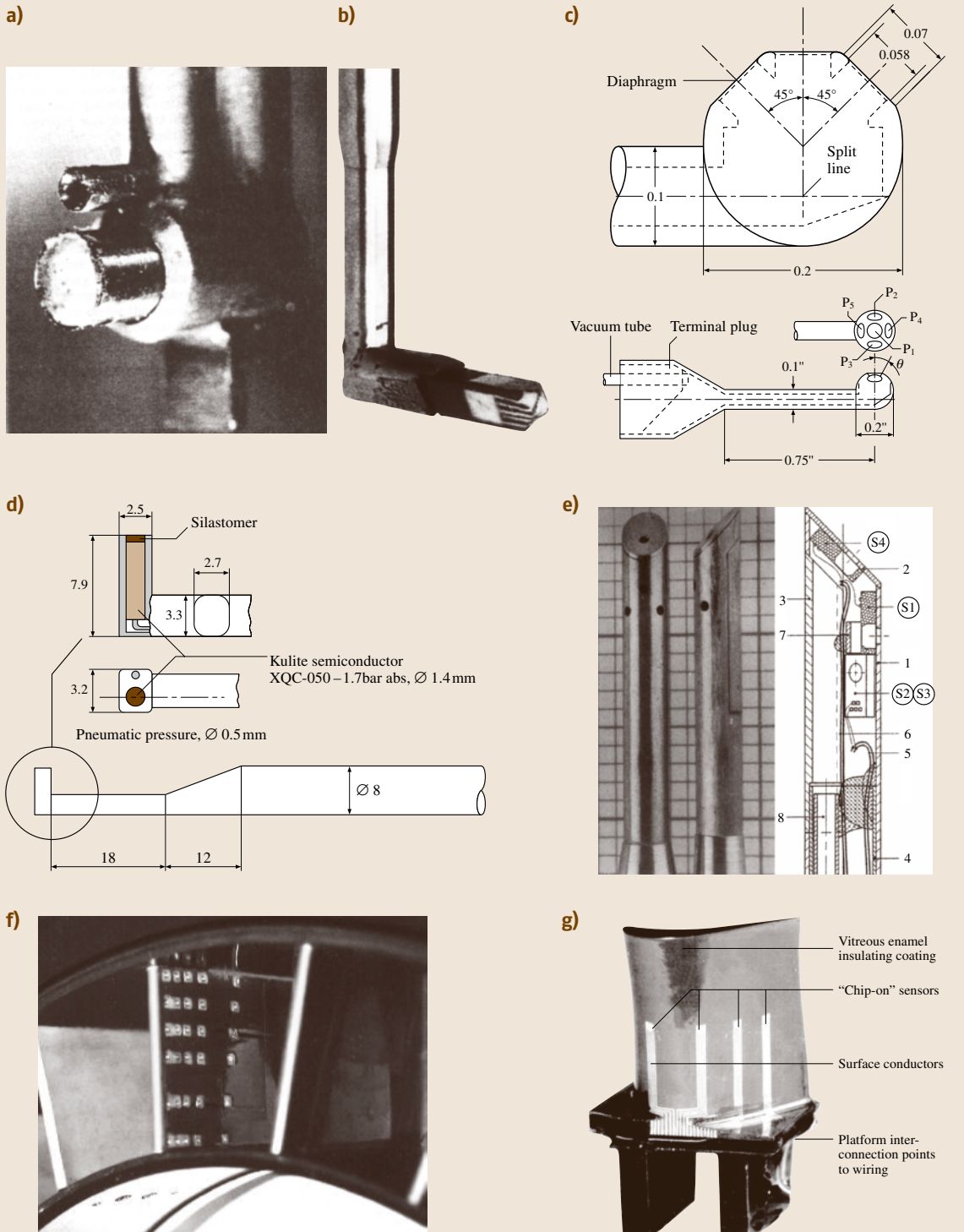
#### Pitot Pressure Probes

Figure 14.5 shows the characteristic configurations of Pitot pressure probes that have been used in turboma-

chinery flow field investigations, and Tables 14.2 and 14.4 provide references for sample studies that have utilized them. A classical reference on this topic is Sitaram et al. [14.84]. Some sensors can only measure the total pressure, such as the wedge, spherical and flat-nosed pitot probes as well as the Kiel probe. The latter is particularly suitable in situations where the flow direction is unknown. Other sensors can measure the total and/or static pressure, such as the conventional Pitot-static (Prandtl) probe and the spherical-head total-static probe, which is insensitive to the flow direction. The three-hole cobra probe, the three-hole Conrad yawmeter probe and the five-hole probe are mostly used for measuring the flow velocity vector in addition to the total and static pressures. The thin three-hole disk-type probe can be used for two-dimensional boundary-layer measurements [14.84]. Most Pitot pressure probes inherently have a low-frequency response. Therefore, they have been used either for measurements in a rotating frame of reference or in measurements within nonrotating inlet guide vanes (IGV) and stator blade passages to obtain the mean flow characteristics.

As suggested by Table 14.2, the five-hole probe has been the most commonly used pressure probe.

**Fig. 14.7a–g** Sample high-frequency-response pressure probes and surface-mounted sensors used in turbomachinery flow investigations: **(a)** Cherrett and Bryce [14.57]. **(b)** Ainsworth et al. [14.58]. **(c)** Kerrebrock et al. [14.54] **(d)** Tiedemann and Kost [14.65]. **(e)** Gossweiler et al. [14.90]. **(f)** Leger et al. [14.68]. **(g)** Ainsworth et al. [14.91]►





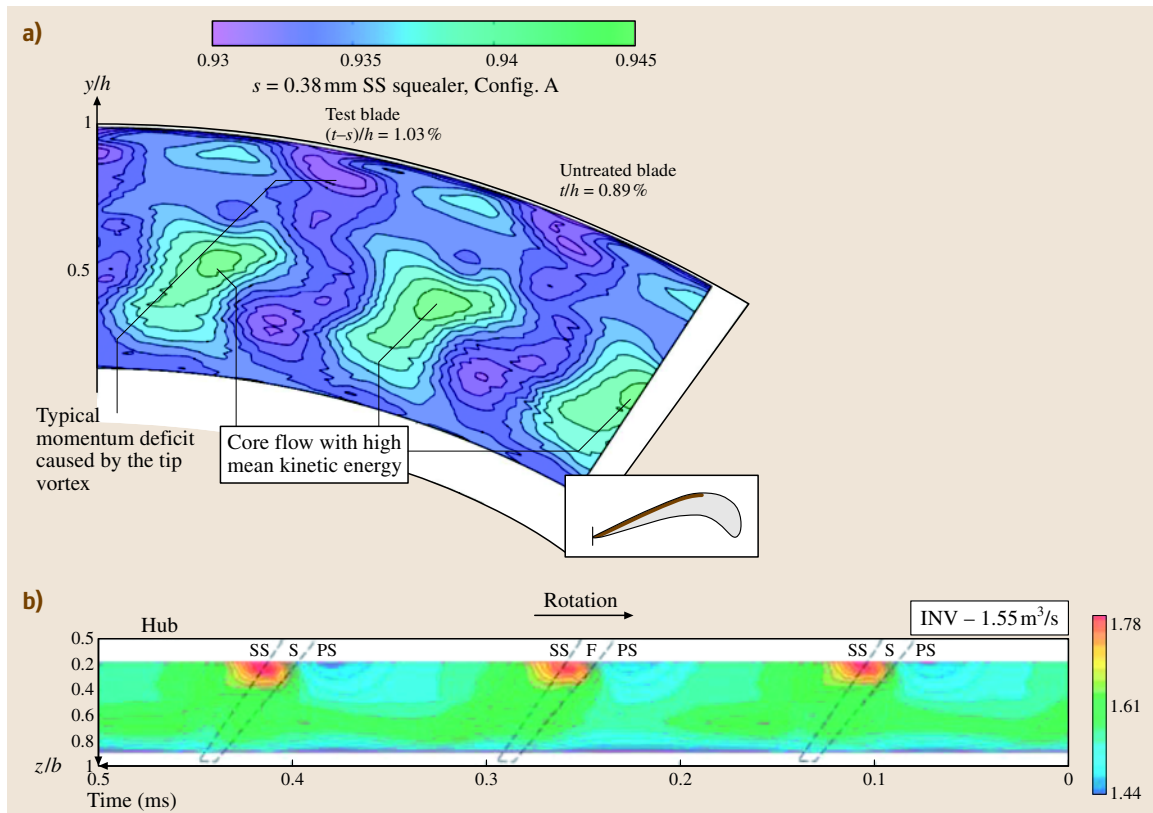


**Fig. 14.8a,b** Sample high-frequency-response pressure probe measurement results (a)  $P_0/P_{in}$  contours downstream of an axial flow turbine rotor (Camci et al. [14.71]) and (b) total pressure ratio contours at the exit of the impeller of a centrifugal compressor (Schleer et al. [14.70])

The five measured pressures are converted to the local total and static pressures as well as the local pitch and yaw angles of the velocity vector, based on calibration. The local mean velocity magnitude is determined from the measured total and static pressures. The five-hole probe is sensitive to Reynolds number, wall vicinity, blockage, and turbulence effects. Detailed information about calibration and data-acquisition procedures for the five-hole probe can be found in Treaster and Yocum [14.83], Lakshminarayana [14.9] and Sitaram et al. [14.84]. Sample results of measurements performed using five-hole probe are presented in Fig. 14.6.

#### High-Frequency-Response Pressure Probes and Sensors

High-frequency pressure probes and surface pressure transducers have been used for measuring unsteady pressure fluctuations in both rotating and stationary

frames of references. They typically have one or more piezoresistive (i.e., a strain-gauge attached to a diaphragm) or piezoelectric (piezoelectric crystal, typically silicon) pressure sensors, that are installed flush-mounted either within a probe or on a blade surface. The natural frequency of these sensors can extend to 150–400 kHz. Comprehensive reviews on applications of high-frequency pressure sensors to turbomachinery flow fields can be found in Sieverding et al. [14.92] and Ainsworth et al. [14.91]. Characteristic samples are listed in Tables 14.3 and 14.4. Most studies have utilized commercially available sensors produced by, e.g., Kulite, Endevco, Entran, PCB, and several others. Mounting of several sensors to a probe head to measure the total and static pressure simultaneously significantly increases the probe head size, although miniature MEMS-based transducers mounted on the tip of the probe have been introduced to remedy this problem [14.93]. Due to interference of the probe with the

flow, *Kupferschmied* et al. [14.94] note that the measured pressures do not, in general, correspond to the total or static pressure of the undisturbed flow, but may be converted into them (and into flow angles and velocity) by calibrations under well-controlled flow conditions.

Figure 14.7 shows several types of probes and surface sensors that have been used in turbomachines, and Fig. 14.8 presents sample results obtained in a stationary reference frame analyzed using the ensemble-averaging technique [14.70, 71].

## 14.3 Optical Measurement Techniques

Optical measurement techniques are typically non-intrusive, and can be implemented within rotating blade passages without having to use rotating probes (although rotating optical probes exist). The primary challenge in applications of optical sensors is to provide appropriate optical access to the flow field within the machine. Laser Doppler velocimetry (LDV) and particle image velocimetry (PIV) have been the most commonly used techniques for measuring velocity and turbulence within turbomachines. LDV has been widely in use since

the early 1970s, whereas PIV was introduced in the late 1980s, but has become popular in turbomachinery applications in the late 1990s. Another optical technique, laser two-focus velocimetry (L2F), has also been used in several studies, but less frequently. Other techniques, such as Doppler global velocimetry (DGV), are still under development. All the aforementioned techniques rely on measurements of the displacement of seed particles. In applications involving airflow, where the particles cannot be neutrally buoyant, they must

**Table 14.5** Sample studies that have used laser Doppler velocimetry (LDV) technique in investigating different aspects of turbomachinery flow fields. (S: stationary frame measurement, R: rotating frame measurement)

Laser Doppler velocimetry (LDV)					
Author(s)	Year	Type	Type of machine	Subject of study	Ref. frame
Wisler and Mossey [14.95]	1973	1-D	Axial compressor	Relative flow field	S
Strazisar [14.96]	1985	1-D	Axial fan rotor	Transonic flow structure	S
Pierzga and Wood [14.97]	1985	1-D	Axial fan rotor	3-D flow field	S
Murthy and Lakshminarayana [14.98]	1986	1-D	Axial compressor	Tip flow field	S
Beaudoin et al. [14.99]	1992	2-D	Centrifugal pump	Effects of orbiting impeller	S
Stauter [14.100]	1993	3-D	Axial compressor	Tip flow field	S
Hathaway et al. [14.101]	1993	3-D	Centrifugal compressor	3-D flow structure	S
Farrell and Billet [14.102]	1994	—	Axial pump	Tip vortex cavitation	S
Abramian and Howard [14.103]	1994	1-D	Centrifugal impeller	Unsteady flow	R
Fagan and Fleeter [14.104]	1994	1-D	Centrifugal compressor	Flow Structure	S
Hobson et al. [14.105]	1996	2-D	Axial compressor cascade	Effect of inlet turbulence	S
Zaccaria and Lakshminarayana [14.106]	1997	2-D	Axial turbine	Wake/blade interaction	S
Adler and Benyamin [14.107]	1999	2-D	Axial turbine	Stator wake transport	S
Ristic et al. [14.108]	1999	3-D	Axial turbine	3-D flow field	S
Kang and Thole [14.109]	2000	3-D	Axial turbine cascade	Endwall flow structure	S
Faure et al. [14.110]	2001	2-D	Axial compressor	Flow Structure	S
McCarter et al. [14.48]	2001	3-D	Axial turbine	Tip clearance effects	S
VanZante et al. [14.111]	2002	2-D	Axial compressor	Blade/row interaction	S
Woistschlager et al. [14.112]	2002	2-D	Axial turbine cascade	Turbine blade wakes	S
Xiao and Lakshminarayana [14.113]	2002	3-D	Axial turbine	Endwall flow structure	S
Matsunuma and Tsutsui [14.114]	2003	2-D	Axial turbine	Unsteady flow	S
Ibaraki et al. [14.115]	2003	2-D	Centrifugal compressor	Transonic flow structure	S
Gottlich et al. [14.85]	2004	2-D	Axial turbine	Stator–rotor interaction	S
Faure et al. [14.116]	2004	3-D	Axial compressor	3-D flow and turbulence structure	S



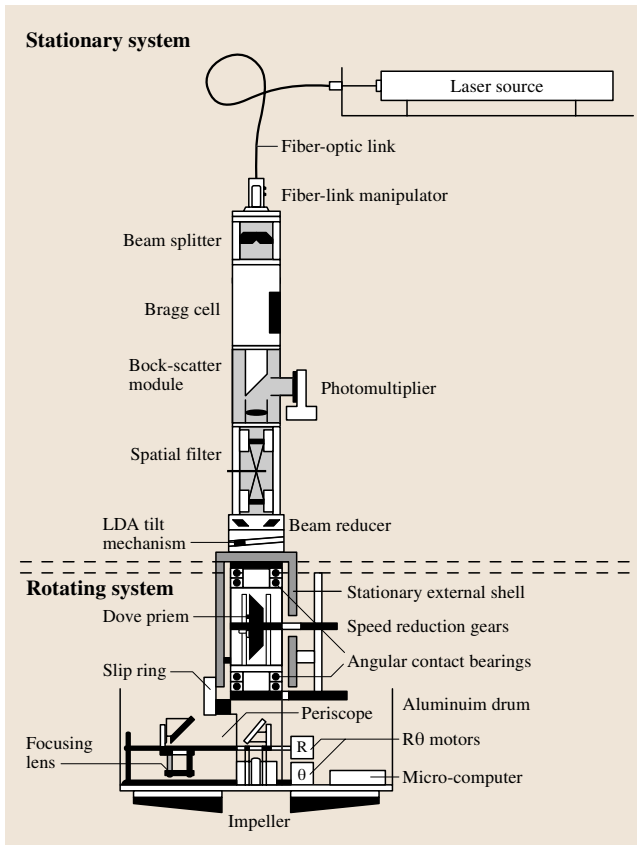


**Fig. 14.9** Schematic of the stationary to rotating frame optical transfer system for relative frame LDV measurements within a centrifugal impeller (Abramian and Howard [14.103])

The operating principles of this technique are well documented in the literature [14.87, 117]. This technique attracted the attention of experimentalists in turbomachinery research soon after it was introduced in 1960s. In addition to being non-intrusive, it allowed measuring the relative velocity and turbulence fields within rotating blade rows, without having to use complex rotating probe traverse and data-transmission mechanisms. Sample studies that have used LDV for measurements within turbomachines are provided in Table 14.5.

Implementation of LDV to turbomachinery flows comes with a variety of problems. For example, due to the inherent accessibility limitations, LDV system must operate in backscatter mode, which reduces the signal-to-noise ratio by one to three orders of magnitude compared to the forward-scatter mode, depending on the particles properties [14.118]. The signal-to-noise ratio is further reduced due to reflections of the incident laser beams near end-wall regions. In addition, the three-dimensional shapes of rotor blades create shadow zones, especially near the hub regions, which necessitate use of complicated off-axis measurement systems. Another critical issue is the optical distortions to the multiple laser beams caused by the curvature of the access windows. These distortions increase the uncertainty of the measurements by deforming the measurement volume and changing the measurement location [14.101]. Doukelis et al. [14.119] estimated the changes in the orientation and relative position of measurement volume due to the window curvature for a three-dimensional (3-D) LDV system. They also proposed a mathematical method to correct for refractions from windows, which could be incorporated into data-acquisition procedures.

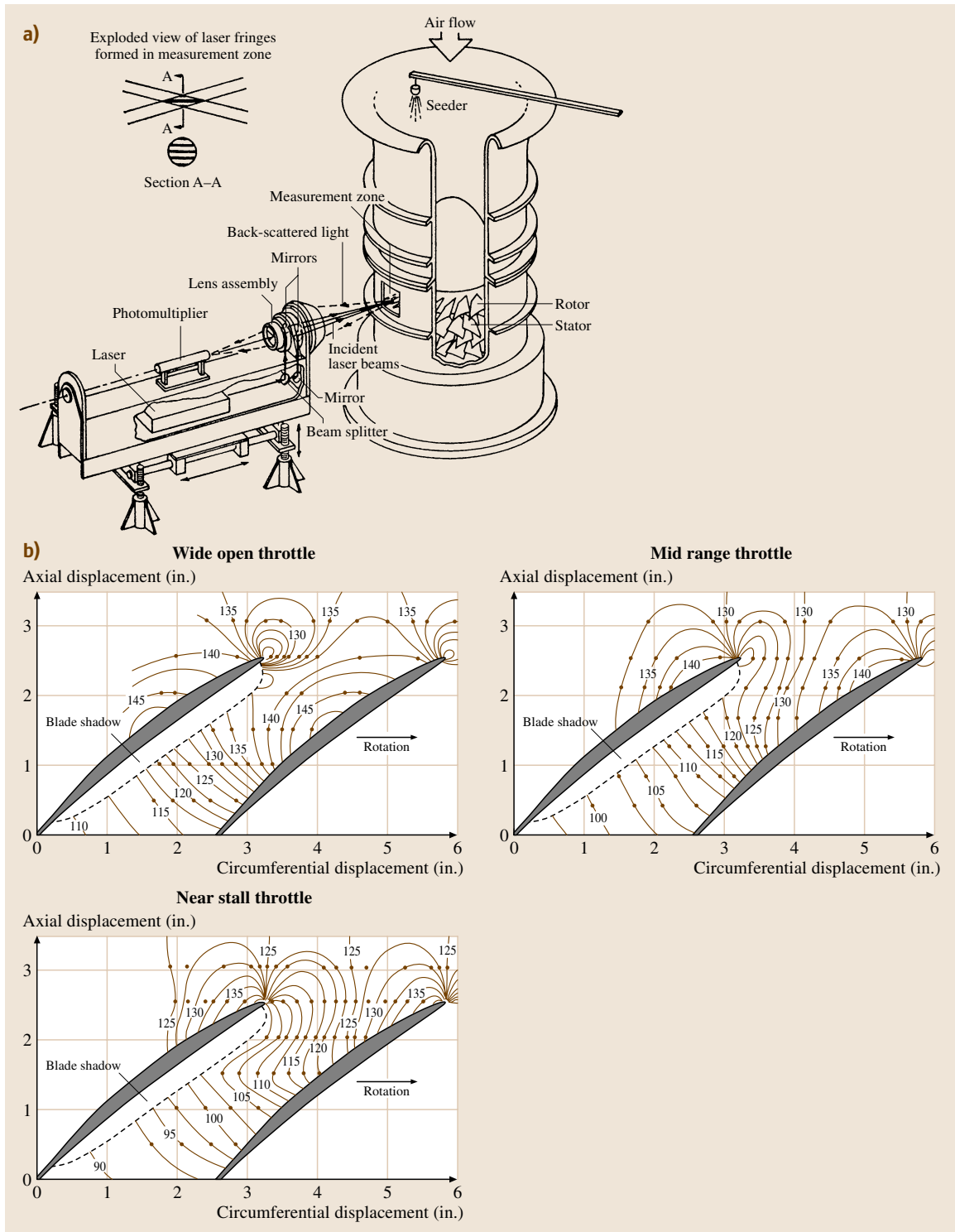
Most investigations involving LDV have been performed in a stationary frame of reference by discretizing the rotor passage period into bins, each with a finite time interval, and ensemble-averaging the results over these bins. To obtain sufficient convergence in mean velocity and turbulence parameters, one would like to increase the number of points per bin. However, increasing the bin size incorporates effects of spatial variations

be kept small enough to follow the fluid motion, especially in areas with very high pressure gradients, such as in shock waves. Consequently, the typical particle size should be around  $0.5\ \mu\text{m}$  to obtain a tolerable velocity lag. In applications involving liquid, the specific gravity of the particle can be better matched with that of the fluid, and significantly larger particles, in the order of  $5\text{--}20\ \mu\text{m}$  can be tolerated, depending on the characteristic flow scales. Non-intrusive pressure distributions measurements on blade surfaces have been performed using pressure-sensitive paint (PSP). This section introduces and provides samples of applications of these techniques in turbomachinery flow fields.

### 14.3.1 Applications of Laser Doppler Velocimetry (LDV)

Laser Doppler velocimetry measures the fluid velocity by detecting the Doppler frequency shift of the laser light that is scattered by small particles moving with the fluid.

**Fig. 14.10a,b** The LDV setup (a) and measured relative velocity contours within the rotor passage of a low-speed research compressor (b) (Wisler and Mossey [14.95])►



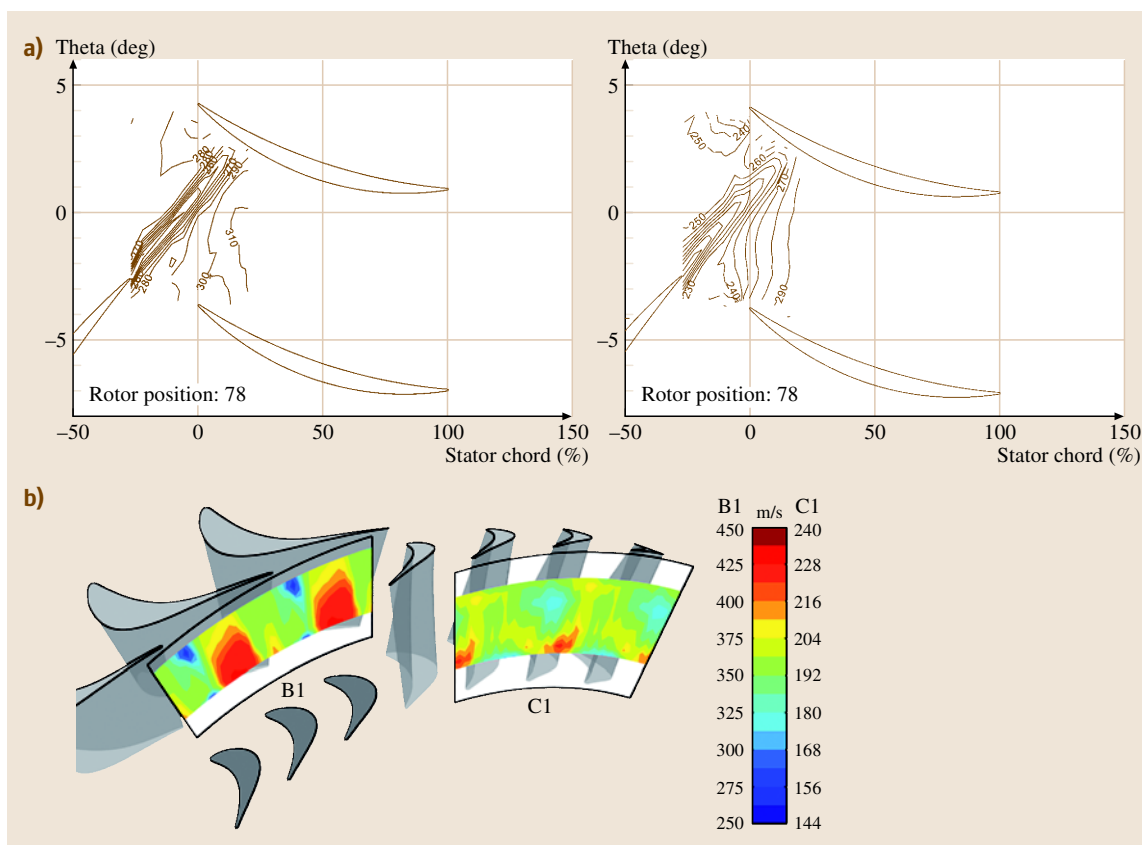
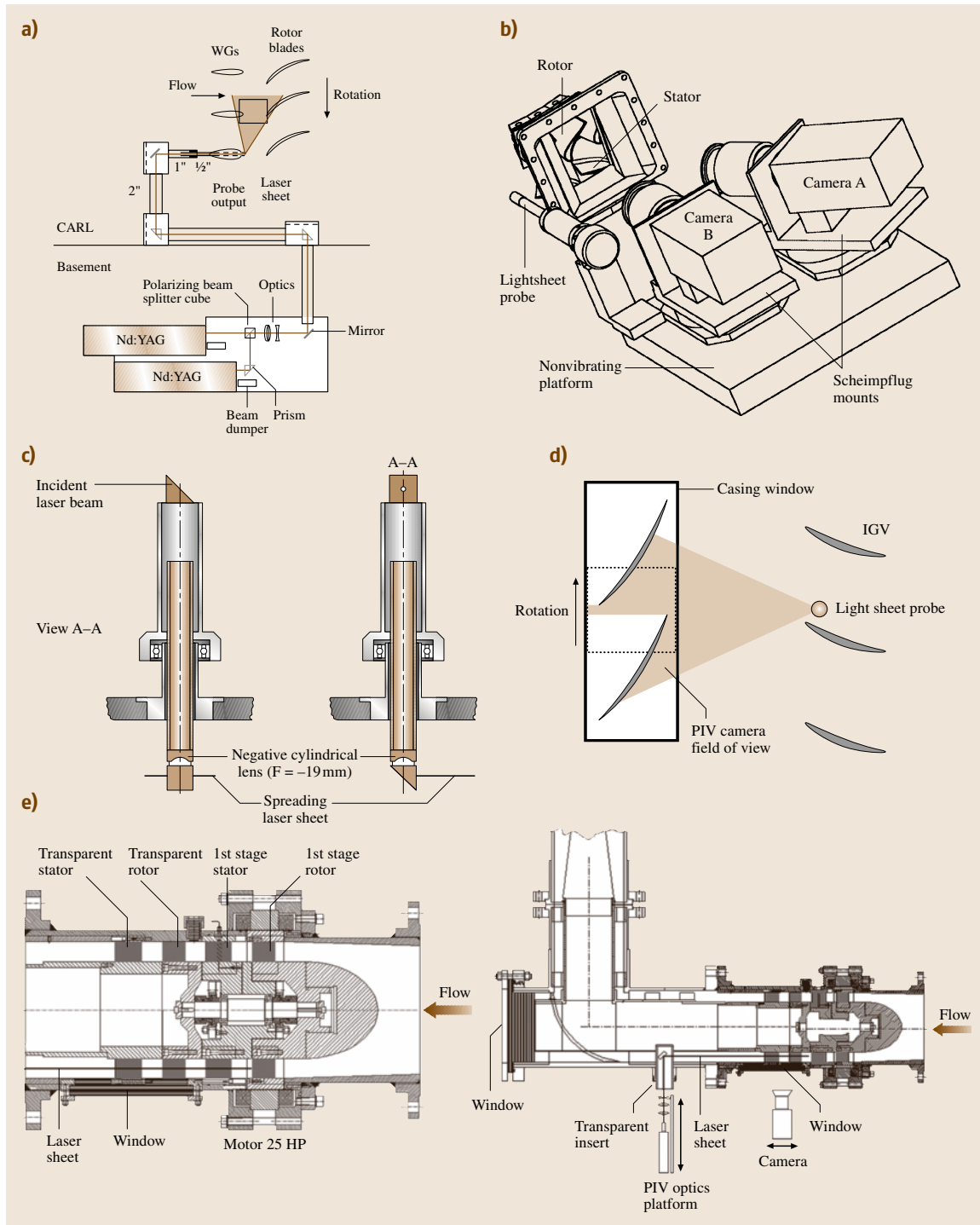


**Fig. 14.11a,b** Sample results from LDV measurements within (a) an axial compressor, rotor wake relative velocity magnitude at peak efficiency (left) and near stall (right) (Van Zante et al. [14.111]) and (b) an axial turbine, time-averaged flow field at the nozzle and rotor exits (Gottlich et al. [14.85])

in the flow structure within the rotor passage into the ensemble-averaged statistics. A discussion on this issue recommending a bin size of 50 points for measurements in an axial flow turbine can be found in Ristic et al. [14.108]. Abramian and Howard [14.103] provided detailed descriptions of mechanical and optical designs for LDV measurements in a rotating frame of reference within a centrifugal impeller. As shown in Fig. 14.9, they used a Dove prism to transfer the laser beams to the rotating frame of reference, along with a rotating periscope, which located the probe volume at any desired point within the blade passage.

As summarized in Table 14.5, one of the earliest applications of LDV to turbomachinery was described by Wisler and Mossey [14.95]. They performed velocity measurements upstream, within and downstream of the first-stage rotor row of an axial compressor, using a single-component system operating in backscatter mode. The flow was seeded by spray-atomizing a dilute water suspension of 1  $\mu\text{m}$ -diameter polystyrene latex particles. Figure 14.11a,b shows their experimental setup and a sample contour plot of relative velocity within the rotor passage at 50% span. Sample results from more-recent applications within an axial compressor

**Fig. 14.12a–e** Sample PIV setups showing the optical access windows and laser and camera positions: (a) axial compressor (Copenhaver et al. [14.120]) WG: “Wake Generator”, (b) axial turbine (Lang et al. [14.121]), (c) optical periscope insert for light-sheet delivery (Balzani et al. [14.122]), (d) schematic of the light-sheet probe and illumination pattern (Wernet et al. [14.123]), (e) index-matched axial pump (Uzol et al. [14.124]) ►



sor [14.111] and within an axial turbine [14.85] are presented in Fig. 14.12.

### 14.3.2 Applications of Particle Image Velocimetry (PIV)

Particle image velocimetry consists of illuminating a flow field seeded with microscopic particles with a thin light sheet, and recording a pair of images, separated by a short time interval. The velocity is determined by dividing the image into small interrogation areas, and using cross-correlation analysis to measure the displacement of particles within each area. This process provides the instantaneous distribution of two in-plane components of the velocity. Stereo imaging using two inclined cameras provides all three components of the velocity in the illuminated plane. Detailed information on technical issues associated with applications of PIV is provided in other chapters of this book. Extensive use of this technology started in the late 1980s and early 1990s [14.125–127]. Further details can be found in a series of papers published in a dedicated volume of *Measurement Science and Technology Journal* [14.128–131]) as well as in a book by Raffel et al. [14.132]. In this section we focus on issues relevant to applications in turbomachinery flows. Table 14.6 provides samples of applications of PIV within turbomachines, which includes also the types of lasers, cameras and particles used in each study. Specific components associated are discussed below. Similar to LDV, the primary challenge in applications of PIV in turbomachines are optical access and reflections from curved and rough boundaries that overwhelm the particle traces.

#### Components and Issues Elated to Implementation

**Lasers.** Similar to other applications, most of the lasers used in turbomachinery studies are frequency-doubled Nd:YAG lasers, with a wavelength of 532 nm, pulse duration of 5–10 ns, and energy of 25–350 mJ/pulse. The sheet thickness varies from about 0.5 to 3 mm. Dual-cavity Nd:YAG lasers allow short pulse-to-pulse separation times that is necessary for high-speed flow measurements. Some early studies have used pulsed copper-vapor lasers [14.133] and high-energy pulsed ruby lasers [14.134].

**Image Acquisition.** In early years, data were recorded on 35 mm films [14.133] or on media like Kodak Technipan [14.134] and then subsequently digitized. With the introduction of digital camera technology with light-

sensitive charged-coupled device (CCD) chips, all PIV studies nowadays collect images in digital form. A variety of cameras with different pixel resolutions from  $640 \times 480$  to  $2048 \times 2048$  pixels<sup>2</sup> have been used. In the so-called *interline transfer* cameras, each pixel is divided to an exposed part that senses the light, and a masked part that serves as a buffer memory. Fast transfer of data from the exposed to masked sections enables the recording of two exposures on separate frames, with an interframe delay of less than 1  $\mu$ s. This approach solves directional ambiguity issues, and provides a high signal-to-noise ratio in correlation analysis. Another approach to achieve short delay between frames is to use *frame-straddling*, i. e., to trigger the first laser pulse at the end of the exposure time of one frame, and the second pulse at the beginning of exposure of the subsequent frame. In a different approach, Esteve et al. [14.135] used a two-color PIV system to resolve the directional ambiguity while investigating the flow field within an axial fan. Their first wavelength, 532 nm, was provided by a frequency-doubled Nd:YAG laser, and the second pulse at 640 nm was generated by using the Nd:YAG laser to pump a dye laser. The images were recorded using a Kodak  $3k \times 2k$  pixels digital camera with a color CCD chip.

**Seeding.** For measurements in axial and centrifugal air compressors and turbines, the particle size is usually less than 1  $\mu$ m. The particles are generated using a variety of methods, such as commercial fog/smoke generators, atomizing glycerin and water/oil mixtures, alumina in ethanol dispersions, etc. In one of the early applications of PIV in turbomachines, which were performed in water, Dong et al. [14.133] used particles containing embedded fluorescent dyes that responded efficiently to green lasers. The specific gravity of these particles varied between 0.95 and 1.1, their size was in the 20–40  $\mu$ m range. By filtering out the green light using a filter placed in front of the camera, they could perform measurements very close to boundaries. Choi et al. [14.136] used nylon 12 particles to investigate the flow field within a centrifugal impeller operating in water. Silver-coated hollow glass particles were used by Uzol et al. [14.124] in an axial pump facility containing a concentrated sodium iodide (NaI) solution for refractive-index-matching purposes, and by [14.137] in a centrifugal rotary blood pump.

**Optical Access.** The flow field in a multistage turbomachine is visually obstructed by the blades, making optical access for the laser sheet and the cameras

**Table 14.6** Sample studies that have used particle image velocimetry (PIV) technique in investigating different aspects of turbomachinery flow fields.

Particle image velocimetry (PIV)				Subject of study	Type of machine	Type	Laser	Camera	Particles
Author(s)	Year								
Paone et al. [14.138]	1989	2-D	Centrifugal pump	Flow structure	Centrifugal pump	2-D	–	–	–
Dong et al. [14.133]	1992	2-D	Centrifugal pump	Flow structure	Centrifugal pump	2-D	Pulsed copper vapor and/or frequency-doubled Nd:YAG, 1 mm thickness	35 mm film and image digitizer	Fluorescent particles
Chu et al. [14.139, 140]	1995	2-D	Centrifugal pump	Unsteady flow and pressure fluctuations	Centrifugal pump	2-D	Pulsed copper vapor and/or frequency-doubled Nd:YAG, 1 mm thickness	35 mm film and image digitizer	Fluorescent particles
Day et al. [14.141]	1996	2-D	Axial turbine	Effect of film cooling on flow structure	Axial turbine	2-D	–	–	–
Tisserant and Breugelmans [14.134]	1997	2-D	Axial compressor	Blade-to-blade flow	Axial compressor	2-D	High-energy pulsed ruby laser, 500 mJ/pulse, 1.5 mm thickness	Camera recording on Kodak Technicalpan 2415	Glycerine oil vapor mixed with air
Dong et al. [14.142]	1997	2-D	Centrifugal pump	Unsteady flow and noise	Centrifugal pump	2-D	Frequency-doubled Nd:YAG, 1 mm thickness	35 mm film and image digitizer	Fluorescent particles
Balzani et al. [14.122]	2000	2-D	Axial compressor	Blade-to-blade flow	Axial compressor	2-D	Frequency-doubled (532 nm) Nd:YAG, 2 mm thickness, 200 mJ/pulse	640 × 480 RS-170 CCD cross-correlation camera	Glycerine oil vapor mixed with air
Sinha and Katz [14.143]	2000	2-D	Centrifugal pump	Flow structure and turbulence	Centrifugal pump	2-D	Nd:YAG, 25 mJ/pulse	2048 × 2048 pixels <sup>2</sup>	Fluorescent particles
Estevadeordal et al. [14.135]	2000	2-D	Axial fan	Flow characteristics	Axial fan	2-D	Frequency-doubled (532 nm) and pumped-dye (640 nm) Nd:YAGs, 1 mm thickness, 60 mJ/pulse	3k × 2k Kodak color CCD	Glycerin and water mixture sub-micron particles
Wernet [14.144]	2000	2-D	Centrifugal compressor	Diffuser flow structure	Centrifugal compressor	2-D	Frequency-doubled (532 nm) Nd:YAG, 1 mm thickness, 200 mJ/pulse	1k × 1k pixels <sup>2</sup>	pH-stabilized dispersion of alumina in ethanol
Wernet [14.145]	2000	2-D	Axial and centrifugal compressor	Technique and flow structure	Axial and centrifugal compressor	2-D	Frequency-doubled (532 nm) Nd:YAG, 1 mm thickness, 200 mJ/pulse	1k × 1k pixels <sup>2</sup>	Smoke and pH stabilized dispersion of alumina in ethanol
Wernet et al.[14.146]	2001	2-D	Centrifugal compressor	Surge	Centrifugal compressor	2-D	Frequency-doubled (532 nm) Nd:YAG, 1 mm thickness, 200 mJ/pulse	1k × 1k pixels <sup>2</sup>	pH-stabilized dispersion of alumina in ethanol
Uzol and Camci [14.147]	2001	2-D	Axial turbine cascade	Trailing edge coolant ejection	Axial turbine cascade	2-D	Frequency-doubled (532 nm) Nd:YAG, 1 mm thickness, 50 mJ/pulse	1k × 1k Kodak ES 1.0	Rosco fog generator

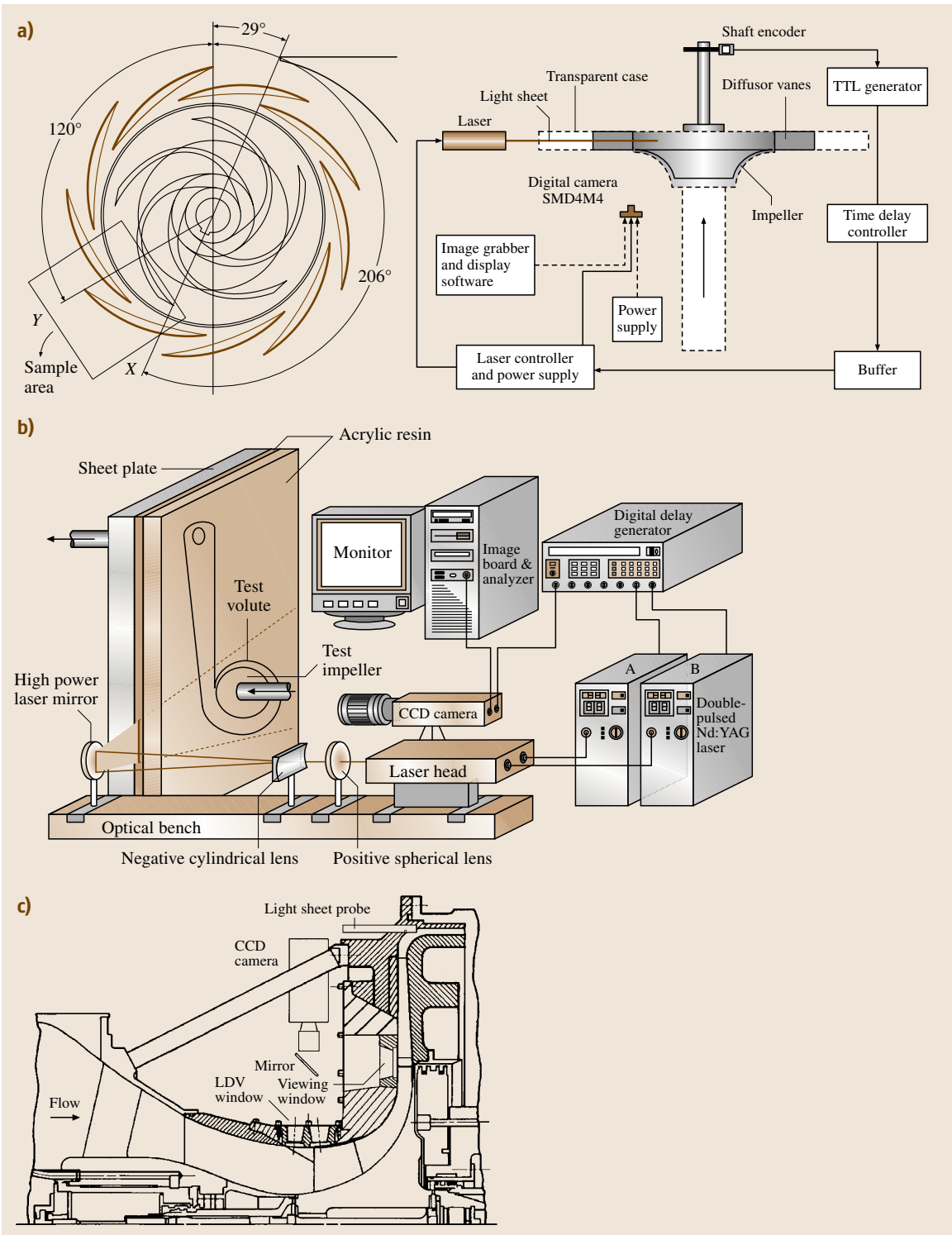
Table 14.6 (continued)

Particle image velocimetry (PIV)							
Author(s)	Year	Type	Type of machine	Subject of study	Laser	Camera	Particles
<i>Sinha</i> et al. [14.148]	2001	2-D	Centrifugal pump	Rotating stall	Nd:YAG, 350 mJ/pulse	2048 × 2048 pixels <sup>2</sup>	Fluorescent particles
<i>Sanders</i> et al. [14.149]	2002	2-D	Axial compressor	Blade–row interactions	Frequency-doubled (532 nm) Nd:YAG, 1 mm thickness, 30 mJ/pulse	1k × 1k Kodak ES 1.0	Rosco fog generator
<i>Wernet</i> et al. [14.123]	2002	3-D	Axial compressor	Tip clearance flow	Frequency-doubled (532 nm) Nd:YAG, 200 mJ/pulse	1k × 1k pixels <sup>2</sup>	Rosco fog generator
<i>Lang</i> et al. [14.121]	2002	3-D	Axial turbine	Rotor–stator interaction	Frequency-doubled (532 nm) Nd:YAG, 2 mm thickness, 120 mJ/pulse	1280 × 1024 pixels <sup>2</sup> CCD (DANTEC 80C60)	Diethylexylsebacat particles, 0.3 μm
<i>Uzol</i> et al. [14.124]	2002	2-D	Axial pump	Flow structure and techniques	Frequency-doubled (532 nm) Nd:YAG, 1 mm thickness, 50 mJ/pulse	2k × 2k Kodak ES 4.0	Silver-coated hollow glass spheres
<i>Uzol</i> et al. [14.150]	2002	2-D	Axial pump	Unsteady flow and deterministic stresses	Frequency-doubled (532 nm) Nd:YAG, 1 mm thickness, 50 mJ/pulse	2k × 2k Kodak ES 4.0	Silver-coated hollow glass spheres
<i>Chow</i> et al. [14.151]	2002	2-D	Axial pump	Wake–wake interactions	Frequency-doubled (532 nm) Nd:YAG, 1 mm thickness, 50 mJ/pulse	2k × 2k Kodak ES 4.0	Silver-coated hollow glass spheres
<i>Copenhaver</i> et al. [14.120]	2002	2-D	Axial compressor	Wake–rotor interaction near stall	Frequency-doubled (532 nm) Nd:YAG, 1 mm thickness	1k × 1k Kodak ES 1.0	Glycerin and water mixture sub-micron particles
<i>Estevadeordal</i> et al. [14.152]	2002	2-D	Axial compressor	Wake–blade interactions	Frequency-doubled (532 nm) Nd:YAG, 1 mm thickness	1k × 1k Kodak ES 1.0	Glycerin and water mixture sub-micron particles
<i>Uzol</i> et al. [14.153]	2003	2-D	Axial pump	Deterministic stresses	Frequency-doubled (532 nm) Nd:YAG, 1 mm thickness, 50 mJ/pulse	2k × 2k Kodak ES 4.0	Silver-coated hollow glass spheres
<i>Chow</i> et al. [14.154]	2003	2-D	Axial pump	Rotor wake structure	Frequency-doubled (532 nm) Nd:YAG, 1 mm thickness, 50 mJ/pulse	2k × 2k Kodak ES 4.0	Silver-coated hollow glass spheres
<i>Woitschlag</i> et al. [14.155]	2003	2-D	Axial turbine cascade	Turbine wake	Frequency-doubled (532 nm) Nd:YAG, 2 mm thickness, 120 mJ/pulse	1280 × 1024 pixels <sup>2</sup> CCD (DANTEC 80C60)	Diethylexylsebacat particles, 0.3 μm
<i>Uzol</i> et al. [14.156]	2004	3-D	Axial pump	3-D wake structure and tip vortex	Frequency-doubled (532 nm) Nd:YAG, 1 mm thickness, 120 mJ/pulse	2k × 2k Kodak ES 4.0	Silver-coated hollow glass spheres



Table 14.6 (continued)

Particle image velocimetry (PIV)		Type	Type of machine	Subject of study	Laser	Camera	Particles
Author(s)	Year						
<i>Uzol</i> et al. [14.157]	2004	3-D	Axial pump	Deterministic stresses	Frequency-doubled (532 nm) Nd:YAG, 1 mm thickness, 120 mJ/pulse	2k × 2k Kodak ES 4.0	Silver-coated hollow glass spheres
<i>Liu</i> et al. [14.158]	2004	3-D	Axial compressor	Tip flow field	Frequency-doubled (532 nm) Nd:YAG, 150 mJ/pulse	1280 × 1024 pixels <sup>2</sup> CCD	Smoke generator
<i>Soranna</i> et al. [14.159]	2004	2-D	Axial pump	Wake–boundary layer interaction	Frequency-doubled (532 nm) Nd:YAG, 1 mm thickness, 120 mJ/pulse	2k × 2k Kodak ES 4.0	Silver-coated hollow glass spheres
<i>Lee</i> et al. [14.160]	2004	3-D	Marine propeller	Propeller wake	Frequency-doubled (532 nm) Nd:YAG, 3 mm thickness, 125 mJ/pulse	1024 × 1024 pixels <sup>2</sup> CCD	Silver-coated hollow glass spheres
<i>Sankovic</i> et al. [14.137]	2004	2-D	Rotary blood pump	Flow structure	Frequency-doubled (532 nm) Nd:YAG, 0.37 mm thickness, 50 mJ/pulse	768 × 484 pixels <sup>2</sup> crosscorrelation camera	Silver-coated hollow glass spheres
<i>Choi</i> et al. [14.136]	2004	2-D	Centrifugal impeller	Flow structure	Frequency-doubled (532 nm) Nd:YAG, 0.5 mm thickness, 20 mJ/pulse	1300 × 1030 pixels <sup>2</sup> CCD	Nylon 12 particles, 30 µm
<i>Chow</i> et al. [14.161]	2005	2-D	Axial pump	Rotor wake, Large Eddy Simulation (LES) modelling	Frequency-doubled (532 nm) Nd:YAG, 1 mm thickness, 120 mJ/pulse	2k × 2k Kodak ES 4.0	Silver-coated hollow glass spheres
<i>Soranna</i> et al. [14.162]	2005	2-D	Axial pump	Wake–blade interactions	Frequency-doubled (532 nm) Nd:YAG, 1 mm thickness, 120 mJ/pulse	2k × 2k Kodak ES 4.0	Silver-coated hollow glass spheres



the key challenge in application of PIV in turbomachines. In addition, light reflections from the blade surfaces and end walls adversely affect the quality of images, especially near the boundaries. In applications involving air flows and realistic geometries, these problems seem to be unavoidable. As a result, most PIV data obtained in multistage turbomachines have covered limited areas, located away from boundaries and mostly between blade rows (see Table 14.6 for references). Characteristic setups for axial air turbomachines used by *Copenhaver et al.* [14.120], *Lang et al.* [14.121], *Balzani et al.* [14.122] and *Wernet et al.* [14.123] are presented in Figs. 14.12a-d. In almost all axial turbomachine applications, the laser sheet has been introduced using periscopic optical inserts (Figs. 14.12c,d), which are located upstream or downstream of the measurement domain, and attached to traverses that enable measurements at different spanwise planes. The cameras view the illuminated plane through windows installed on the outer casing, which are curved internally to match the contour of the machine.

Examples of various PIV setups for measurements within centrifugal turbomachinery, and referenced in Table 14.6, are presented in Fig. 14.13. In most applications, the sample area has been illuminated using side windows [14.136, 143] or inserted probes [14.146]. In a recent study, *Estevadeordal et al.* [14.163] introduced a fiber-optic PIV system that could be used in flows without a direct optical access, and implemented it to measure the flow within an axial turbine.

To resolve the limited access problem, *Uzol et al.* [14.124] and *Chow et al.* [14.151] have introduced a refractive-index-matched liquid facility that enabled unobstructed PIV measurements within an entire stage by matching the optical index of refraction of the blades with that of the working fluid, a concentrated solution of NaI in water ( $\approx 64\%$  by weight). This method not only made it possible to obtain complete optical access to an entire stage, it also minimized the light reflection from boundaries as well, allowing high-resolution measurements of blade boundary layers. The optical setup of this system is illustrated in Fig. 14.12e. A miniature refractive-index-matching facility made entirely from transparent material was also used recently by *Sankovic*

*et al.* [14.137] to measure the flow structure within a centrifugal rotary blood pump.

**Data Acquisition.** Although high-speed PIV systems have started to appear in recent years, a common typical turbomachinery PIV system with low-frame-rate cameras cannot be used to obtain time-resolved flow field measurements. To obtain phase-locked data at specific phase of the rotor blade-passing period, a signal obtained from a shaft encoder is fed to a digital delay generator, which then triggers the lasers and the cameras. Multiple instantaneous measurements obtained at a specific phase are ensemble-averaged to obtain the phase-averaged flow and turbulence parameters. The database should be sufficiently large to obtain converged statistics. In many previous applications, 100 and 1000 samples have been shown to provide converged phase-averaged and turbulence quantities, respectively [14.164, 165]. However, it is essential to check convergence in individual applications. By averaging phase-locked data obtained over many phases, which are distributed evenly over an entire cycle, one can determine the *average-passage* or time-mean flow structure. Any averaging of a flow field introduces stresses, and time averaging of phase-locked data introduces the deterministic stresses [14.166, 167]. A detailed discussion on how to calculate the spatial distributions of deterministic stresses within a turbomachine based on PIV data obtained in discrete phases can be found in *Sinha et al.* [14.168] and *Uzol et al.* [14.150], [14.153].

### Samples of Results

Figures 14.14–14.17 show selected sample results of both two-dimensional and stereoscopic PIV measurements performed within various axial and centrifugal turbomachinery facilities. A more-extended set of references is provided in Table 14.6. A two-dimensional, phase-averaged relative velocity vector map measured at 70% span within the transonic axial compressor facility at the NASA Glenn Research Center [14.145] is presented in Fig. 14.14a. Shock waves attached to the rotor leading edge of blades are clearly visible. Figure 14.14b shows the unsteady 2-D velocity field within the stator passages of the transonic research compressor facility at Purdue University [14.149]. These results were used to investigate the decay of upstream rotor wakes as they are convected through the stator passages. Figure 14.14c presents multiplane two-dimensional data, showing the spanwise variation of the rotor relative velocity within the axial compressor facility at the Von Karman Institute [14.122]. Figure 14.14d presents stereoscopic

**Fig. 14.13a–c** Sample PIV setups for centrifugal turbomachinery: (a) centrifugal pump (*Sinha and Katz* [14.143]); (b) centrifugal impeller (*Choi et al.* [14.136]); (c) centrifugal compressor (*Wernet et al.* [14.146]) ◀

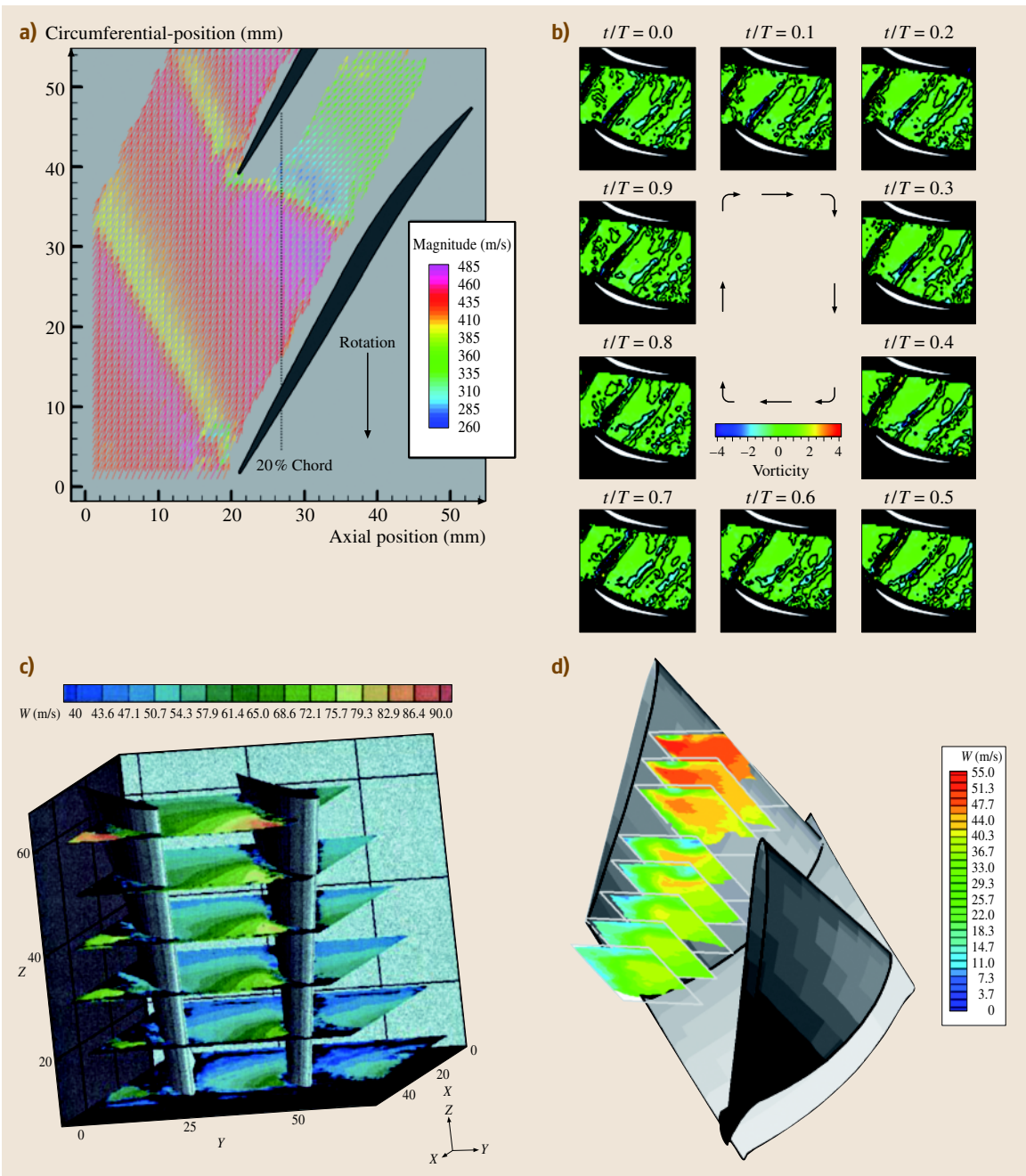


**Fig. 14.14** (a) Velocity distribution within a transonic compressor (Wernet et al. [14.145]) with colors indicating the vector magnitude; (b) unsteady vorticity field within a stator passage (Sanders et al. [14.149]); (c) rotor relative velocity field from hub to tip (Balzani et al. [14.122]); (d) average radial velocity distribution near stall, stereoscopic measurement (Liu et al. [14.158])

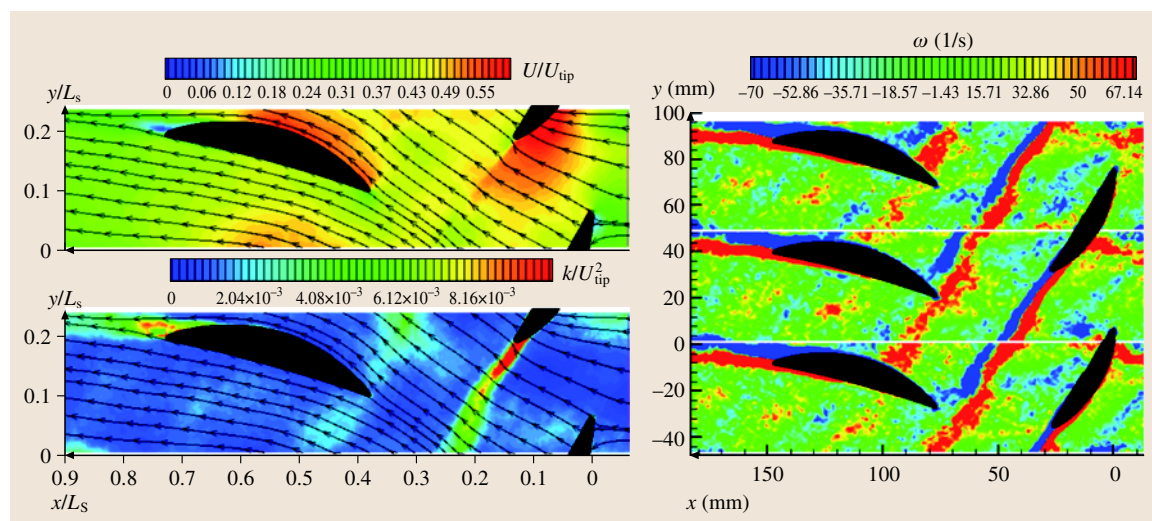


**Fig. 14.15** Sample PIV data obtained in the refractive-index-matched axial pump facility at Johns Hopkins University: phase-averaged velocity field (*top left*), turbulent kinetic energy (*bottom left*) and vorticity (*right*) at mid-span within an entire stage (Chow et al. [14.151])

PIV data of the flow near stall conditions in the low-speed axial compressor facility at Beijing University [14.158]. These measurements provide clear views on the complex, spatially nonuniform flow within axial turbomachines. Yet, in all cases, reflection from the surfaces and limitations in access prevent coverage of the entire stage and prevent measurements close to boundaries. As noted before, in air facilities, the only ones that can examine compressibility effects, these problems are extremely difficult to resolve.

Figures 14.15 and 14.16 present sample results from the two-dimensional and stereoscopic measurements performed in the refractive-index-matched axial turbomachinery facility at Johns Hopkins University. The unobstructed view allowed detailed investigations of wake–blade, wake–wake, wake–boundary layer, and tip vortex–blade interactions in an actual multistage environment. Figure 14.15 shows characteristic distributions of phase-averaged velocity, vorticity and turbulent kinetic energy covering the entire mid-span of a second stage. Data obtained at 10 different phases was used for calculating the distributions of average-passage flow and deterministic stresses (Uzol et al. [14.150, 153]). High-resolution measurements (vector spacing of  $117\mu\text{m}$ ) that required patching of several sample areas were used for characterization of turbulence parameters, including Reynolds and subgrid (SGS) stresses and associated energy fluxes, due to shearing and straining of wakes during pas-

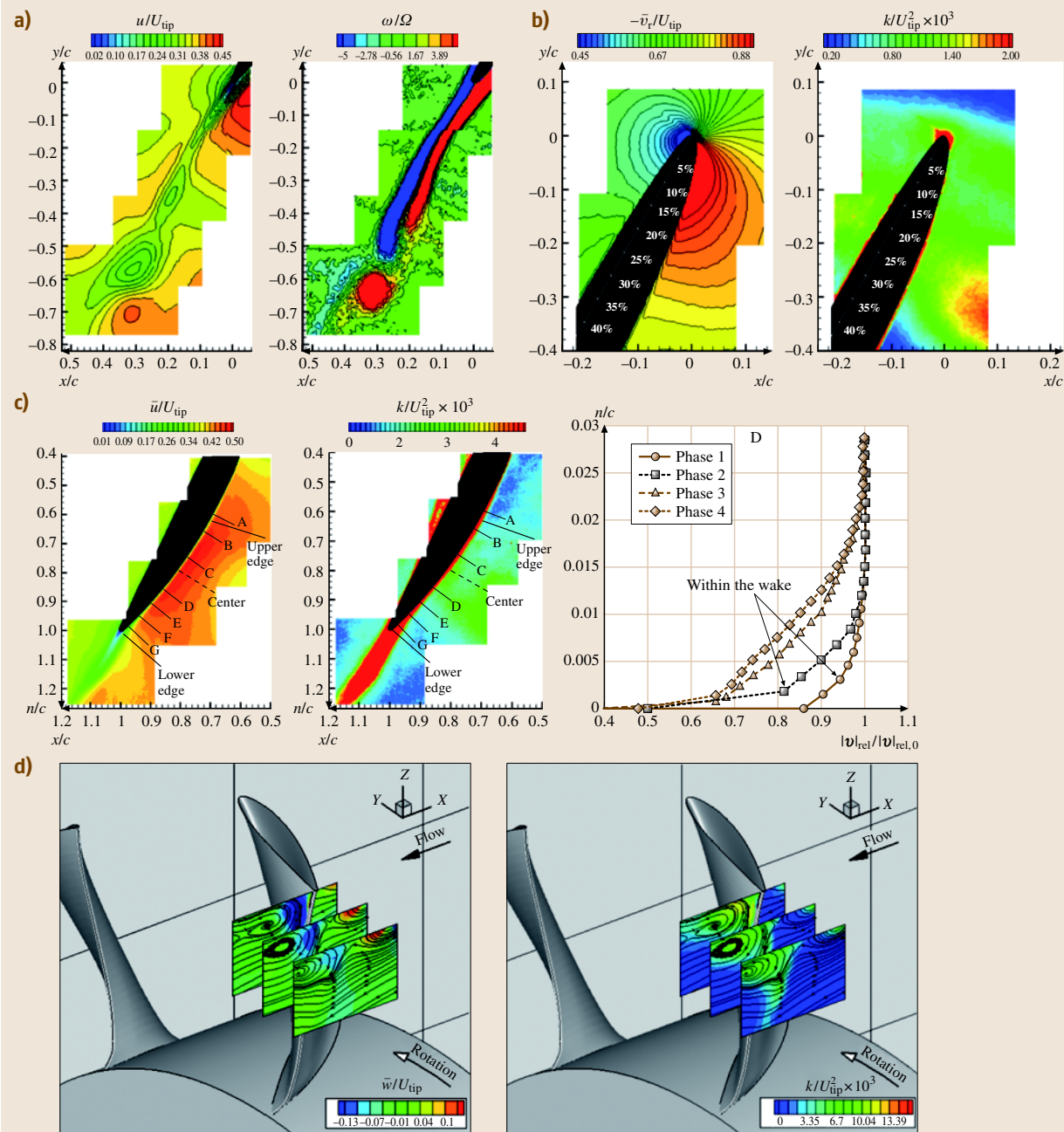
sage in downstream blade rows (Figs. 14.16a,b, Chow et al. [14.151, 154, 161]; Soranna et al. [14.162, 169]). These data were also used to show that unsteady flow caused by upstream wake impingement stabilized the structure of rotor blade boundary layers (Fig. 14.16c, Soranna et al. [14.159]). Samples from stereoscopic measurements in multiple, closely spaced planes, spanwise variations and tip vortex–blade interactions, are presented in Fig. 14.16d.

Figure 14.17a presents sample 2-D PIV data obtained in a centrifugal pump (Fig. 14.13a) seeded with fluorescent particles and filtering of images to eliminate adverse effects of reflections [14.143]. Figure 14.17b shows sample data obtained in a high-speed centrifugal compressor (Fig. 14.13c) operating both at the design point and during surge [14.144, 146].

### 14.3.3 Applications of Laser Two-Focus Velocimetry (L2F)

The L2F technique measures the time of flight of small particles between two highly focused laser spots. Unlike LDV, an instantaneous realization with L2F is generally not a valid measurement, since it is not possible to ensure that the same particle passes through both laser spots. Therefore, L2F has been utilized as a statistics-based measurement device. In typical applications, one of the laser beams is rotated around the other, and many time-of-flight measurements are performed over a range





**Fig. 14.16a–d** PIV measurements in a refractive-index-matched axial pump facility: high-resolution measurements of (a) rotor wake (Chow et al. [14.154]), (b) wake–blade interaction near the rotor leading edge (Soranna et al. [14.162]), (c) wake–boundary layer interactions near the rotor trailing edge (Soranna et al. [14.159]) at midspan, (d) phase-averaged radial velocity (left), and turbulent kinetic energy (right) between 50–93% span, obtained using stereoscopic measurements (Uzol et al. [14.156])

**Table 14.7** Sample studies that have used laser-two-focus velocimetry (L2F) technique in investigating different aspects of turbomachinery flow fields

Laser two-focus velocimetry (L2F)			
Author(s)	Year	Type of machine	Subject of study
McDonald et al. [14.170]	1980	Transonic compressor rotor	Flow structure
Fagan and Fleeter [14.104]	1994	Low-speed centrifugal compressor	Flow structure
Calvert and Stapleton [14.171]	1994	Transonic fan	Flow structure
Ivey and Swoboda [14.43]	1998	Low-speed axial compressor	Tip clearance effects
Kost et al. [14.63]	2000	Axial turbine	Unsteady flow
Ottavy et al. [14.172]	2001	Transonic axial compressor	Wake–shock interaction
Tiedemann and Kost [14.65]	2001	High-pressure axial turbine	Rotor–stator clocking
Schodl et al. [14.173]	2002	Transonic centrifugal compressor	3-D flow structure
Ziegler et al. [14.174]	2003	High-speed centrifugal compressor	Blade–wake interaction

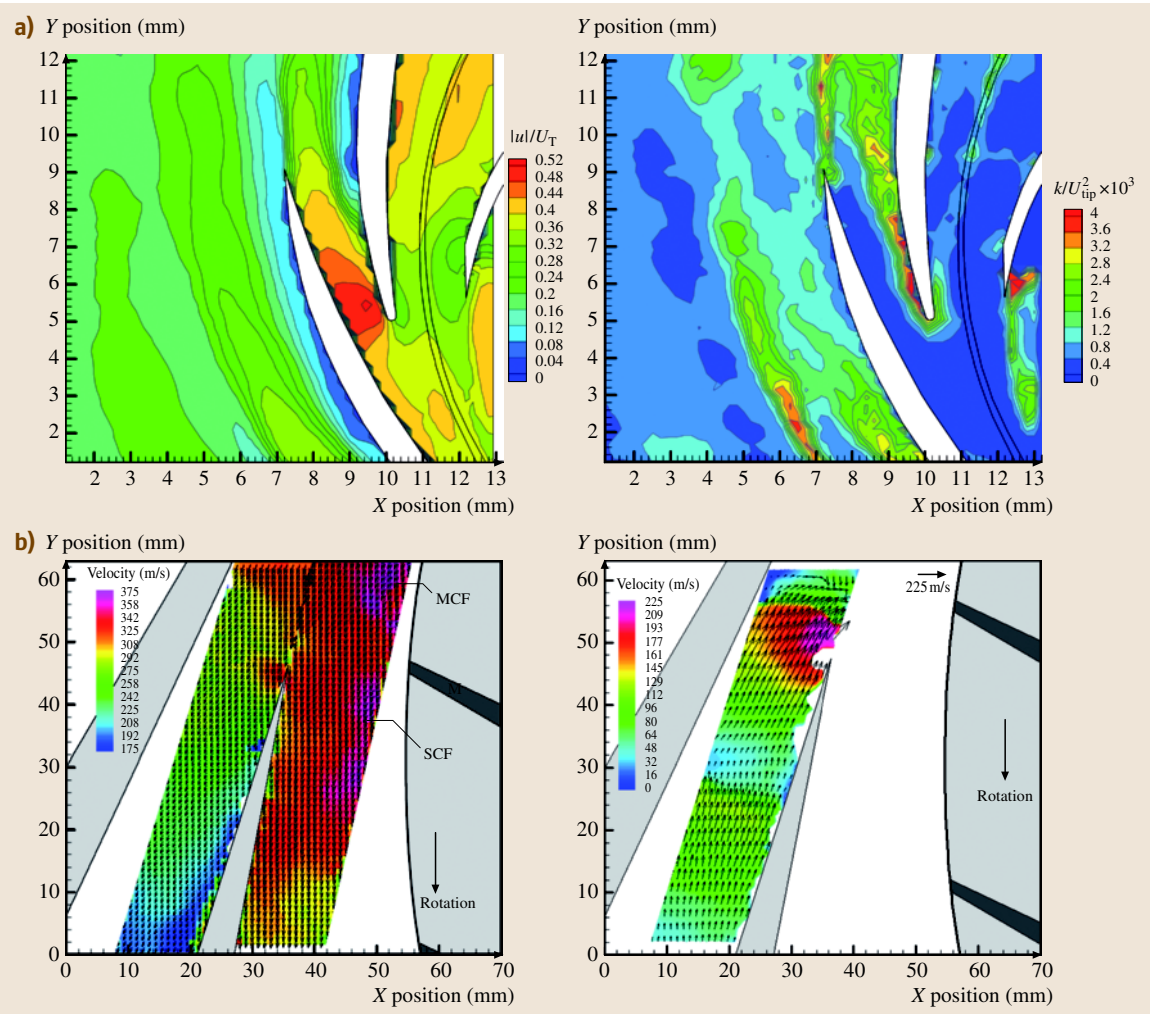


**Fig. 14.17a,b** Sample PIV measurements in a (a) centrifugal pump, phase-averaged velocity (left) and turbulent kinetic energy (right) (Sinha and Katz [14.143]), (b) high-speed centrifugal compressor diffuser velocity vector maps at the design point (left, Wernet [14.144]) and during a surge (right, Wernet et al. [14.146]) MCF: Main Clearance Flow, SCF: Splitter Clearance Flow



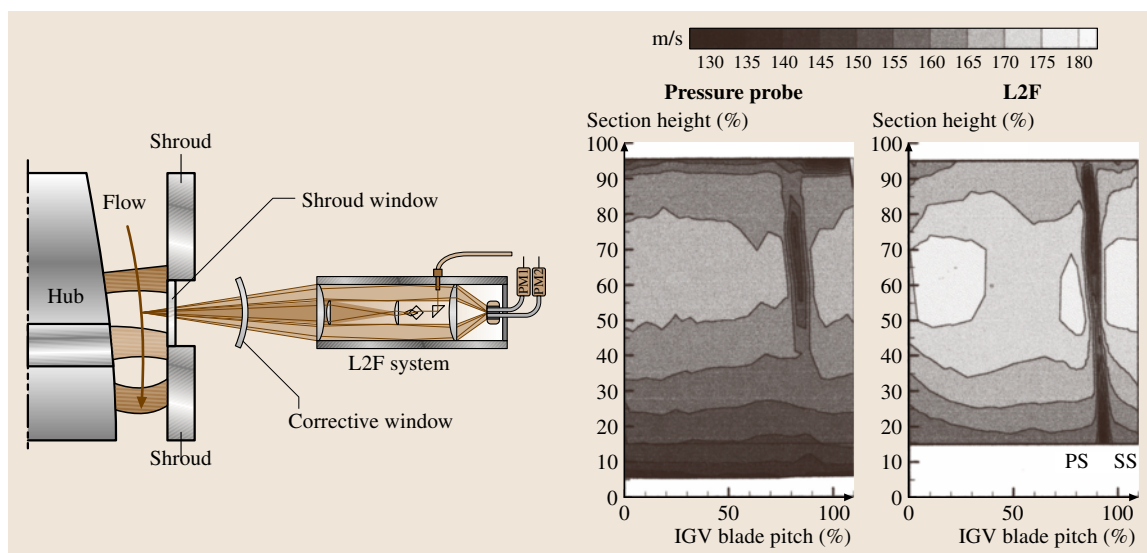


**Fig. 14.18** (a) A sample L2F measurement setup within an axial compressor, and (b) corresponding data compared with three-hole pressure probe measurements (Ottavy et al. [14.172])

of measurement directions. The data produces a two-dimensional probability histogram, which is used to calculate the average velocity and flow angle, along with an estimate of turbulence intensity. Table 14.7 provides a list of sample studies that have used L2F to study flows within turbomachines.

Fagan and Fleeter [14.104] compared the results of LDV and L2F measurements performed within a large-scale, low-speed centrifugal compressor. They found that, although L2F allowed measurements closer to boundaries compared to LDV, the LDV data demonstrated more consistency, in terms of conservation of mass and a reasonable distribution of work. They concluded that LDV would be preferable to L2F due to the latter's low effective sampling rate and upper limits of turbulence intensity. Both they and Schodl [14.177, 178] suggest an upper limit of approximately 15% for accurate turbulence measurements.

Similar to LDV, applications of L2F in turbomachines are adversely affected by optical distortions during the passage of the laser beams through curved optical access windows. The problem is more severe for L2F since the distortions prevent the creation of acceptably focused spots, resulting in a total loss of data. Ottavy et al. [14.179] studied these distortions and proposed a corrective method, which restored the optical focus, and subsequently applied their setup within an axial transonic compressor [14.172]. Figure 14.18 shows their setup, along with a comparison of their L2F data to

results of three-hole pressure probe measurements performed downstream of an IGV and upstream of a rotor row.

Schodl et al. [14.173] introduced a new L2F technique called Doppler laser two-focus velocimeter, and applied it to obtain data within a transonic centrifugal compressor. In this technique, the time-of-flight data was used to measure the velocity vector components in the plane perpendicular to the optical axis. The Doppler shift of the scattered light, as measured using iodine absorption (Sect. 14.3.4), was used to obtain the velocity component along the optical axis, i.e., similar to the Doppler global velocimetry (DGV) technique.

### 14.3.4 Applications of Doppler Global Velocimetry (DGV)

Doppler global velocimetry, also known as planar Doppler velocimetry (PDV), is a planar flow measurement technique, which is based on measuring the Doppler shift of light scattered from tracer particles. The fre-

**Fig. 14.19** (a) Comparison of surface pressure distribution on a rotor suction side in a transonic axial compressor obtained using PSP (left) to CFD predictions (right) (Navarra et al. [14.175]); (b) Experimental setup for PSP measurements in an automotive turbocharger, and (c) pressure distributions on the compressor inlet wall and on the impeller blade (Gregory [14.176]) ►

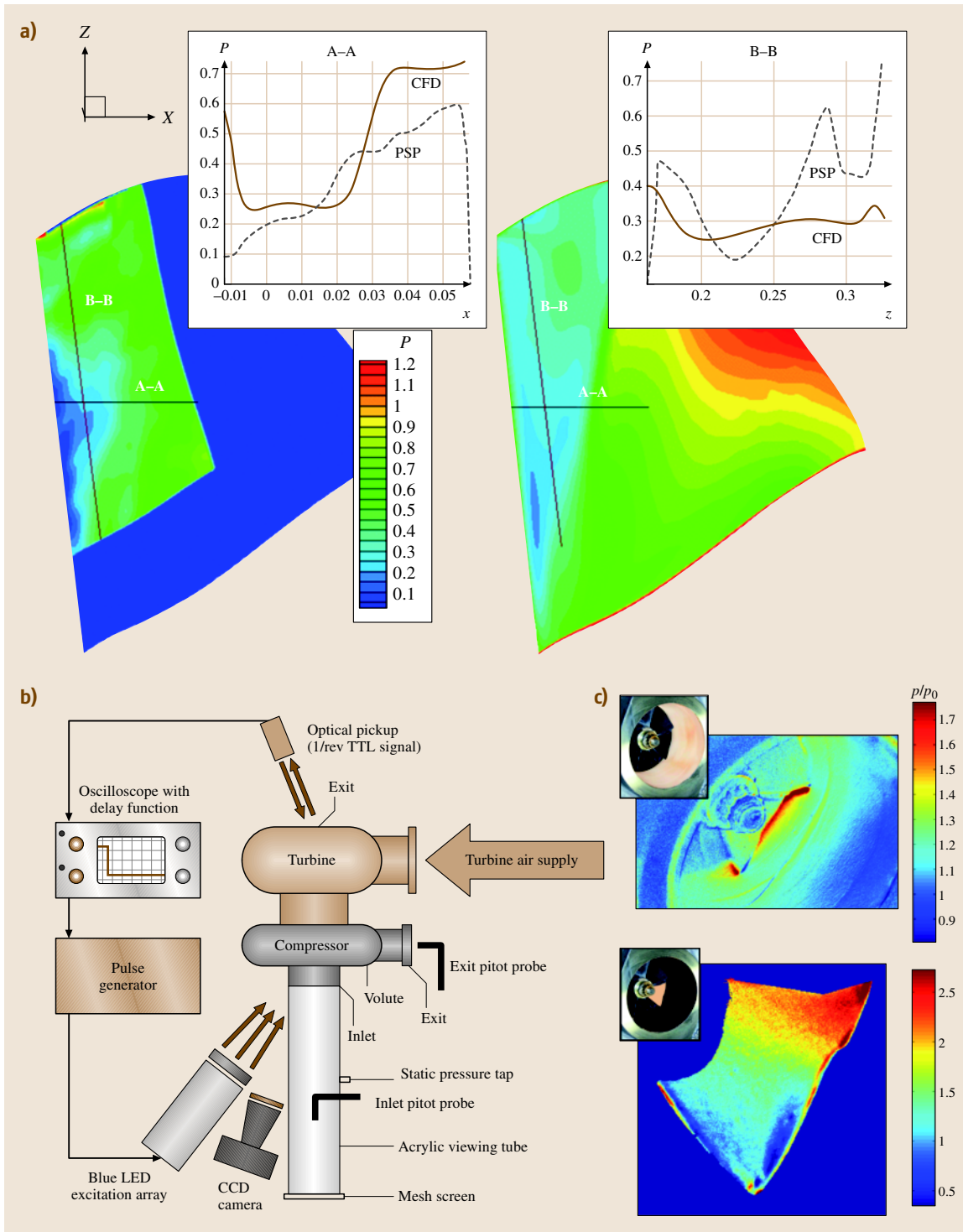


**Table 14.8** Sample studies that have used pressure-sensitive paint (PSP) technique in investigating various aspects of turbomachinery flow fields

Pressure-sensitive paint (PSP)			
Author(s)	Year	Type of machine	Subject of study
Sabroske et al. [14.184]	1995	Axial compressor	Blade pressure distributions
Liu et al. [14.185]	1997	High-speed axial compressor	Blade surface pressure measurements with shocks
Engler et al. [14.186]	2000	Axial turbine	Shock movement and corner stall
Navarra et al. [14.175]	2001	Transonic axial compressor	Blade surface pressure in transonic conditions
Lepicovsky and Bencic [14.187]	2002	Supersonic throughflow fan	Effect of changing operating conditions
Gregory [14.176]	2004	Centrifugal compressor	Effect of inlet distortion on surface pressures

quency shift is measured by means of a frequency–intensity converter, which typically consists of measuring the attenuation of the scattered light as it passes through an iodine-vapor absorption cell [14.180]. This technique is yet to be implemented for turbomachinery flows, but setups designed for turbomachine applications have already been introduced [14.181, 182]. Wernet [14.183] introduced a hybrid PIV/DGV technique and proposed to use it as a viable technique that could be applied to flows with limited optical access, such as turbomachinery flow fields.

14.3.5 Applications of Pressure-Sensitive Paint (PSP)

The current PSP method is based on covering a surface with luminescent coatings that contain sensor molecules embedded in a transparent oxygen-permeable binder. When illuminated by light of appropriate wavelength, the excited sensors molecules emit light at a different wavelength, whose intensity is inversely proportional to the partial pressure of oxygen near the surface. Thus, the intensity of luminescence provides the distribution of surface static pressures. Further details about this technique can be found in a comprehensive review by Bell et al. [14.188]. This method is an attractive alternative to conventional surface pressure measurement techniques since pressure taps or flush-mounted transducers (Sect. 14.2.2) only provide data at discrete points, and are restricted to sites where they can be installed on the blade surfaces. It is typically impossible to in-

strument regions of most interest, such as thin leading edges and sharp corners. Furthermore, many sensors are required to obtain a reasonable spatial distribution, making the measurements time consuming and expensive. PSP provide the spatial distribution of surface pressures at high resolution, enabling measurements of aerodynamic loads on rotor and stator blades. It also serves as a quantitative surface visualization tool that shows the location of shocks, and boundary-layer separation and reattachment points.

Unlike external aerodynamics studies, where PSP is well established, its application to turbomachinery components is rather limited. Sample studies that have used pressure-sensitive paint in turbomachines are summarized in Table 14.8. Selecting two examples, Navarra et al. [14.175] used PSP to measure the pressure distribution on the suction surface of the first stage rotor of a state-of-the-art, full-scale transonic compressor. Figure 14.19a shows a comparison of their data with computational fluid dynamics (CFD) results. Recently, Gregory [14.176] presented results of PSP measurements in the centrifugal compressor of a Garrett T25 turbocharger, which is typically used in automotive applications. Using porous polymer/ceramic PSP they investigated the effect of inlet distortion on the pressure distribution on the surface of blades and on the wall at the inlet to the compressor. Figure 14.19b presents their experimental setup, showing the transparent inlet wall that allowed visual access, the blue light-emitting diode (LED) used to excite the PSP, and the camera that recorded the intensity of luminescence from painted surface. Figure 14.19b shows the unsteady wall pressure distribution on the inlet wall (top) and on the impeller blade (bottom).

14.4 Concluding Remarks

This chapter attempts to provide a comprehensive but brief summary of measurement techniques that have been used for studying flows within turbomachines.

Being focused on techniques, we discuss issues that are unique to applications of various sensors in such a complex flow environment. For each class of sen-

sors, a table provides examples of applications, along with sample results. We also attempt to include examples of implementation in various types of machines, e.g., axial and centrifugal compressors and pumps, large and small facilities, full-scale devices and small-scale models. However, one should bear in mind that one cannot cover more than 50 years of experimental studies of flow within turbomachines in a single chapter, or in a single book for that matter. The reader should refer to the several books mentioned in the introduction for a more-comprehensive treatment of the fluid-mechanics and heat-transfer problems within turbomachines. Besides serving as samples, the cited references can also

be used as starting points for more-detailed searches on specific topics. As is evident, the level of sophistication of instruments as well as the size of database and level of detail that they can resolve has been increasing rapidly over the years, in part in response to the challenge posed by the rapid advancements in CFD tools. The ever-increasing levels of detail revealed by recent multipoint flow measurement tools enable us to elucidate and quantify complex interactions between multiple flow features, which is characteristic to turbomachines. The resulting insights are essential both for validation of predicted flows, as well as for challenging the modeling community to continue addressing discrepancies.

## References

- 14.1 J.H. Horlock: *Axial Flow Compressors* (Kreiger Publishing Co., Melbourne FL 1973)
- 14.2 J.H. Horlock: *Axial Flow Turbines* (Kreiger, Melbourne FL 1973)
- 14.3 A.T. Sayers: *Hydraulic and Compressible Flow Turbomachines* (McGraw-Hill, Berkshire 1990)
- 14.4 E. Logan Jr.: *Turbomachinery: basic theory and applications* (Marcel Dekker, New York 1993)
- 14.5 B. Lakshminarayana: *Fluid Dynamics and Heat Transfer Turbomachin* (Wiley, New York 1996)
- 14.6 J.A. Schetz, A.E. Fuhs: *Handbook of Fluid Dynamics and Fluid Machinery* (Wiley, New York 1996)
- 14.7 S.L. Dixon: *Fluid Mechanics and Thermodynamics of Turbomachinery 4th edition*, 4th edn. (Butterworth-Heinemann, Woburn 1998)
- 14.8 D.G. Wilson, T. Korakianitis: *The Design of High-Efficiency Turbomachinery and Gas Turbines 2nd edition* (Prentice-Hall, Upper Saddle River 1998) (looseness!)
- 14.9 B. Lakshminarayana: Techniques for aerodynamic and turbulence measurements in turbomachinery rotors, *J. Eng. Power* **103**(2), 374–392 (1981)
- 14.10 V.S.P. Chaluviadi, A.I. Kalfas, M.R. Banieghbal, H.P. Hodson, J.D. Denton: Blade-Row Interaction in a High Pressure Turbine, *J. Propulsion Power* **17**(4), 892–901 (2001)
- 14.11 J.R. Weske: An investigation of the aerodynamic characteristics of a rotating axial flow blade grid, NACA Technical Note **1128** (1947)
- 14.12 C.A. Gorton, B. Lakshminarayana: A method of measuring the three-dimensional mean flow and turbulence quantities inside a rotating turbomachinery passage, *J. Eng. Power Ser. A* **98**(2), 137–146 (1976)
- 14.13 B. Reynolds, B. Lakshminarayana, A. Ravindranath: Characteristics of the near wake of a compressor of a fan rotor blade, *AIAA J.* **17**(9), 959–967 (1979)
- 14.14 R.P. Dring, H.D. Joslyn: Measurement of turbine rotor blade flows, *J. Eng. Power* **103**, 400–405 (1981)
- 14.15 H.D. Joslyn, R.P. Dring: Three-dimensional flow in an axial turbine: Part 1 – Aerodynamic Mechanisms, *J. Turbomachin.* **114**(1), 61–70 (1992)
- 14.16 B. Lakshminarayana, A. Poncet: A Method of Measuring Three-Dimensional Wakes in Turbomachinery, *J. of Fluids Eng., J. Fluids* **96**(2), 87–91 (1974)
- 14.17 C. Hah, B. Lakshminarayana: Freestream Turbulence Effects on the Development of a Rotor Wake, *AIAA J.* **19**(6), 724–730 (1980)
- 14.18 B. Lakshminarayana, T.R. Govindan, B. Reynolds: Effects of rotation and blade incidence on properties turbomachinery rotor wake, *AIAA J.* **20**(2), 245–253 (1982)
- 14.19 Y. Dong, N.A. Cumpsty: Compressor blade boundary layers: Part 2 – Measurements with incident wakes, *J. Turbomachin.* **112**(2), 231–240 (1990)
- 14.20 H.P. Hodson, I. Huntsman, A.B. Steele: An Investigation of Boundary Layer Development in a Multi-stage LP Turbine, *J. Turbomachin.* **116**(3), 375–383 (1994)
- 14.21 T.R. Camp, H.W. Shin: Turbulence intensity and length scale measurements in multistage compressors, *J. Turbomachin.* **117**(1), 38–46 (1995)
- 14.22 A.S. Witkowski, T.J. Chmielniak, M.D. Strozik: Experimental study of a 3D wake decay and secondary flows behind a rotor blade row of a low speed compressor stage, *ASME* **96-GT-415** (1996)
- 14.23 D.E. Halstead, D.C. Wisler, T.H. Okiishi, G.J. Walker, H.P. Hodson, H.W. Shin: Boundary layer development in axial flow compressors and turbines: Part 1 – composite picture, *J. Turbomachin.* **119**(1), 114–127 (1997)
- 14.24 S.T. Hsu, A.M. Wo: Near-wake measurement in a rotor/stator axial compressor using slanted hot-wire technique, *Exp. Fluids* **23**(5), 441–444 (1997)

- 14.25 A. Sentker, W. Riess: Measurement of unstead flow and turbulence in a low speed axial compressor, *Exp. Therm. Fluid Sci.* **17**, 124–131 (1998)
- 14.26 D. Ristic, B. Lakshminarayana: Three-dimensional blade boundary layer and endwall flow development in the nozzle passage of a single stage turbine, *J. Fluids Eng.* **120**, 570–579 (1998)
- 14.27 J. Prato, B. Lakshminarayana, N. Suryavamshi: Steady and unsteady three-dimensional flow field downstream of an embedded stator in a multi-stage axial flow compressor: Part 1 – unsteady velocity field, *ASME* **98-GT-521** (1998)
- 14.28 M. Furukawa, K. Saiki, K. Nagayoshi, M. Kuroumaru, M. Inoue: Effect of stream surface inclination on tip leakage flow fields in compressor rotors, *J. Turbomachin.* **120**(4), 683–394 (1998)
- 14.29 A. Sentker, W. Riess: Experimental investigation of turbulent wake-blade interaction in axial compressors, *Int. J. Heat Fluid Flow* **21**, 285–290 (2000)
- 14.30 S. Velarde-Suarez, R. Ballasteros-Tajadura, C. Santolaria-Morros, J. Gonzalez-Perez: Unsteady flow pattern characteristics downstream of a forward-curved blades centrifugal fan, *J. Fluids Eng.* **123**, 265–270 (2001)
- 14.31 Y.H. Shin, R.L. Elder, I. Bennett: Boundary layer measurement on the blade surface of a multi-stage axial flow compressor, *Proc. ASME Turbo Expo 2003* (ASME, Atlanta 2003)
- 14.32 C. McLean: *The Aerodynamic Effects of Wheel-space Coolant Injection into the Mainstream Flow of a High Pressure Gas Turbine*, Ph.D. Dissertation (Pennsylvania State University, University Park 2000)
- 14.33 W.F. O'Brien Jr., H.L. Moses, H.R. Carter: Multi-channel telemetry system for flow research on turbomachine rotors, *ASME* **74-GT-112** (1974)
- 14.34 R.W. Light: *Development of rotating to stationary data transfer system based on FM telemetry*, M.S. Thesis, Mechanical Engineering (Virginia Poly. Inst. And State Univ., Blacksburg 1975)
- 14.35 A. Adler: Telemetry for Turbomachinery, *Mech. Eng.* **101**(3), 30–35 (1979)
- 14.36 J.G.B. Worthy: The design, development and operation of gas turbine radio telemetry system, *J. Eng. Power* **103**(2), 473–479 (1981)
- 14.37 A. Zeisberger, L. Matziol, F. Deubert: Modern telemetry systems and rotating instrumentation, *Proc. ASME Turbo Expo 2002* (Amsterdam 2002)
- 14.38 J. Neustein: Low Reynolds number experiments in an axial-flow turbomachine, *J. Eng. Power*, 257–295 (1964)
- 14.39 S. Kang, C. Hirsch: Experimental study on the three-dimensional flow within a compressor cascade with tip clearance: Part 1 – The Tip Leakage Vortex, *J. Turbomachin.* **115**(3), 444–451 (1993)
- 14.40 J.F. Carotte, K.F. Young, S.J. Stevens: Measurement of the flow field within a compressor outlet guide vane passage, *J. Turbomachin.* **117**, 29–37 (1995)
- 14.41 J. Prato, B. Lakshminarayana, N. Suryavamshi: Exit flow field of an embedded stator in a multi-stage axial flow compressor, *J. Propulsion Power* **113**(2), 169–177 (1997)
- 14.42 A. Doukelis, K. Mathioudakis, K. Papailiou: The effect of tip clearance gap size and wall rotation on the performance of a high-speed annular compressor cascade, *ASME* **98-GT-38** (1998)
- 14.43 P.C. Ivey, M. Swoboda: Leakage effects in the rotor tip clearance region of a multi-stage axial compressor: Part 1 – Innovative Experiments, *ASME* **98-GT-591** (1998)
- 14.44 D. Dey, C. Camci: Development of tip clearance flow downstream of a rotor blade with coolant injection from a tip trench, *Proc. International Symposium on Rotating Machinery-ISROMAC* (Honolulu 2000)
- 14.45 X. Xiao, A.A. McCarter, B. Lakshminarayana: Tip clearance effects in a turbine rotor: Part 1 – pressure field and loss, *J. Turbomachin.* **123**(2), 296–304 (2001)
- 14.46 C. McLean, C. Camci, B. Glezer: Mainstream aerodynamic effects due to wheel-space coolant injection in a high pressure turbine stage: Part 1 – aerodynamic measurements in the stationary frame, *J. Turbomachin.* **123**(4), 687–696 (2001)
- 14.47 C. McLean, C. Camci, B. Glezer: Mainstream aerodynamic effects due to wheel-space coolant injection in a high pressure turbine stage: Part 2 – aerodynamic measurements in the rotational frame, *J. Turbomachin.* **123**(4), 697–703 (2001)
- 14.48 A.A. McCarter, X. Xiao, B. Lakshminarayana: Tip clearance effects in a turbine rotor: Part 2 – velocity field and flow physics, *J. Turbomachin.* **123**(2), 305–313 (2001)
- 14.49 S. Coldrick, P. Ivey, R. Wells: Considerations for using 3-D pneumatic probes in high speed axial compressors, *J. Turbomachin.* **125**(1), 149–154 (2003)
- 14.50 G. Pullan, J.D. Denton, M. Dunkley: An experimental and computational study of the formation of a streamwise shed vortex in a turbine stage, *J. Turbomachin.* **125**(2), 291–297 (2003)
- 14.51 J.L. Gilarranz, A.J. Ranz, J.A. Kopko, J.M. Sorokes: On the Use of Five-Hole Probes in the Testing of Industrial Centrifugal Compressors, *J. Turbomachin.* **127**(1), 91–106 (2005)
- 14.52 D.M. Boyd, S. Fleeter: Axial compressor blade-to-blade unsteady aerodynamic variability, *J. Propulsion Power* **19**(2), 242–249 (2003)
- 14.53 V.S.P. Chaluvadi, A.I. Kalfas, H.P. Hodson: Vortex Transport and Blade Interactions in High Pressure Turbines, *J. Turbomachin.* **126**(3), 395–405 (2004)
- 14.54 J.L. Kerrebrock, A.H. Epstein, W.T. Thompkins Jr.: Miniature high frequency sphere probe, *Proc. Joint Fluids Eng. Gas Turbine Conf.* (New Orleans 1980)
- 14.55 W.T. Cousins, W.F.J. OBrien, M.R. Sexton: *Dynamic pressure response with stall on axial flow compressor rotor blades*, *AIAA 1981-69, 19th AIAA Aerospace Sciences Meeting 1981, St. Louis* (AIAA, Reston 1981)



- 14.56 G.L. Giannissis, A.B. McKenzie, R.L. Elder: Experimental investigation of rotating stall in a mis-matched three-stage axial flow compressor, *J. Turbomachin.* **111**(4), 418–425 (1989)
- 14.57 M.A. Cherrett, J.D. Bryce: Unsteady Viscous Flow in a High Speed Core Compressor, *J. Turbomachinery* **114**(2), 287–294 (1992)
- 14.58 R.W. Ainsworth, J.L. Allen, J.J.M. Batt: The development of fast response aerodynamic probes for flow measurements in turbomachines, *J. Turbomachin.* **117**, 625–634 (1995)
- 14.59 M.K. Fabian, E.J. Jumper: *Unsteady pressure distributions around compressor vanes in an unsteady, transonic cascade*, AIAA 1995–302, 33rd AIAA Aerospace Sciences Meeting 1995 (AIAA, Reno 1995)
- 14.60 R. Laborde, P. Chantrel: Tip clearance and tip vortex cavitation in an axial flow pump, *J. Fluids Eng.* **119**, 680–685 (1997)
- 14.61 Y. Dong, B. Lakshminarayana, D. Maddock: Steady and unsteady flow field at pump and turbine exits of a torque converter, *J. Fluids Eng.* **120**, 538–548 (1998)
- 14.62 G. Roduner C.; Koppel P.; Kupferschmied P.; Gyarmathy: Comparison of measurement data at the impeller exit of a centrifugal compressor measured with both pneumatic and fast-response probes, *J. Turbomachin.* **121**(3), 609–618 (1999)
- 14.63 F. Kost, F. Hummel, M. Tiedmann: Investigation of the Unsteady Rotor Flow Field in a Single HP Turbine Stage, ASME Paper 2000–GT–432 (2000)
- 14.64 R. Mailach, I. Lehmann, K. Vogeler: Rotating instabilities in an axial compressor originating from the fluctuating tip vortex, *J. Turbomachin.* **123**(3), 453–463 (2001)
- 14.65 M. Tiedemann, F. Kost: Some Aspects of Wake-Wake Interactions Regarding Turbine Stator Clocking, *J. Turbomachin.* **123**, 526–533 (2001)
- 14.66 H. Lohrberg, B. Stoffel, R. Fortes-Patella, O. Coutier-Delgosha, J.L. Reboud: Numerical and experimental investigation on the cavitating flow in a cascade of hydrofoils, *Exp. Fluids* **33**(4), 578–586 (2002)
- 14.67 M. Nohmi, Y. Iga, A. Goto, T. Ikahagi: Experimental and numerical study of cavitation breakdown in a centrifugal pump, ASME/JSME Joint Fluids Engineering Conference (Honolulu, 2003)
- 14.68 T.J. Leger, D.A. Johnston, J.M. Wolff: Flex circuit sensor array for surface unsteady pressure measurements, *J. Propulsion Power* **20**(4), 754–758 (2004)
- 14.69 Z.S. Spakovszky: Backward travelling rotating stall waves in centrifugal compressors, *J. Turbomachin.* **126**(1), 1–12 (2004)
- 14.70 M. Schleer, S.S. Hong, M. Zangeneh, C. Roduner, B. Ribi, F. Ploger, R.S. Abhari: Investigation of an inversely designed centrifugal compressor stage: Part 2 – experimental investigations, *J. Turbomachin.* **126**(1), 82–90 (2004)
- 14.71 C. Camci, D. Dey, L. Kavurmacioglu: Aerodynamics of tip leakage flows near partial squealer rims in an axial flow turbine stage, *J. Turbomachin.* **127**(1), 14–24 (2005)
- 14.72 R.C. Lockhart, G.J. Walker: The influence of viscous interactions on the flow downstream of an axial compressor stage, *Proc. 2nd Int. Symp. Air Breathing Engines* (Sheffield 1974)
- 14.73 E.M. Greitzer: Surge and rotating stall in axial flow compressors Part 2 – experimental results and comparison with theory, *J. Eng. Power* **98**(2), 199–217 (1976)
- 14.74 D.G. Gregory-Smith, J.G.E. Cleak: Secondary flow measurements in a turbine cascade with high inlet turbulence, *J. Turbomachin.* **114**(1), 173–183 (1992) (looseness1)
- 14.75 I.J. Day: Axial compressor performance during surge, *J. Propulsion Power* **10**(3), 329–336 (1994)
- 14.76 K.H. Kim, S. Fleeter: Compressor unsteady aerodynamic response to rotating stall and surge excitations, *J. Propulsion Power* **10**(5), 698–708 (1994)
- 14.77 H.E. Gallus, J. Zeschky, C. Hah: Endwall and unsteady flow phenomenon in an axial turbine stage, *ASME* **94–GT–143** (1994)
- 14.78 U. Reinmoller, B. Stephan, S. Schmidt, R. Niehuis: Clocking effects in a 15 stage axial turbine—steady and unsteady experimental investigations supported by numerical simulations, *J. Turbomachin.* **124**, 52–60 (2002)
- 14.79 A.J. Sanders, S. Fleeter: Rotor blade-to-blade wake variability and effect on downstream vane response, *J. Propulsion Power* **18**(2), 456–464 (2002)
- 14.80 R.T. Johnston, S. Fleeter: Airfoil row/wake interactions in a high speed axial compressor, *J. Propulsion Power* **18**(6), 1280–1288 (2002)
- 14.81 M.T. Schobeiri, B. Ozturk, D.E. Ashpis: On the physics of flow separation along a low pressure turbine blade under unsteady flow conditions, ASME Turbo Expo 2003 (ASME, Atlanta 2003)
- 14.82 R.T. Johnston, S. Fleeter: Three-dimensional time-resolved inlet guide vane-rotor potential field interaction, *J. Propulsion Power* **20**(1), 171–179 (2004)
- 14.83 A.L. Treaster, A.M. Yocum: The calibration and application of five-hole probes, *ISA Trans.* **18**(3), 23–34 (1979)
- 14.84 N. Sitaram, B. Lakshminarayana, A. Ravindranath: Conventional Probes for the relative flow measurement in a turbomachinery rotor blade passage, *J. Eng. Power* **103**(2), 406–414 (1981)
- 14.85 E. Gottlich, F. Neumayer, J. Woisetschlager, W. Sanz, F. Heitmeir: Investigation of stator-rotor interaction in a transonic turbine stage using laser Doppler velocimetry and pneumatic probes, *J. Turbomachin.* **126**(2), 297–305 (2004)
- 14.86 H.H. Bruun: *Hot-wire Anemometry – Principles and Signal Analysis* (Oxford Univ. Press, New York 1995)

- 14.87 R.J. Goldstein (Ed.): *Fluid Mechanics Measurements* (Taylor Francis, Washington 1996)
- 14.88 L.H. Smith Jr.: Wake dispersion in turbomachines, *J. Basic Eng. Ser. D* **88**(3), 688–690 (1966)
- 14.89 G.J. Walker, A.R. Oliver: The effect of interaction between blade rows in an axial flow compressor on the noise generated by blade interaction, *J. Eng. Power* **94**, 241–248 (1972)
- 14.90 C.R. Gossweiler, P. Kupferschmied, G. Gyarmathy: On fast response probes: Part 1—Technology, calibration and application to turbomachinery, *J. Turbomachin.* **117**(4), 611–617 (1995)
- 14.91 R.W. Ainsworth, R.J. Miller, R.W. Moss, S.J. Thorpe: Unsteady pressure measurement, *Meas. Sci. Technol.* **11**, 1055–1076 (2000)
- 14.92 C.H. Sieverding, T. Arts, R. Denos, J.F. Brouck-aert: Measurement techniques for unsteady flows in turbomachines, *Exp. Fluids* **28**, 285–321 (2000)
- 14.93 L. Lofdahl, M. Gad-el-Hak: MEMS-based pressure and shear stress sensors for turbulent flows, *Meas. Sci. Technol.* **10**(8), 665–686 (1999)
- 14.94 P. Kupferschmied, P. Koppel, W. Gizzi, C. Roduner, G. Gyarmathy: Time-resolved flow measurements with fast-response aerodynamic probes in turbomachines, *Meas. Sci. Technol.* **11**, 1036–1054 (2000looseness1)
- 14.95 D.C. Wisler, P.W. Mossey: Gas velocity measurements within a compressor rotor passage using the laser doppler velocimeter, *J. Eng. Power Ser. A* **95**(2), 91–96 (1973)
- 14.96 A.J. Strazisar: Investigation of flow phenomenon in a transonic fan rotor using laser anemometry, *J. Eng. Gas Turbines Power* **107**, 427–435 (1985)
- 14.97 M.J. Pierzga, J.R. Wood: Investigation of the three-dimensional flow field within a transonic fan rotor: experiment and analysis, *J. Eng. Gas Turbines Power* **107**, 436–448 (1985)
- 14.98 K.N.S. Murthy, B. Lakshminarayana: Laser-Doppler velocimetry measurement in the tip region of a compressor rotor, *AIAA J.* **24**(5), 474–481 (1986)
- 14.99 R.J. Beaudoin, S.M. Miner, R.D. Flack: Laser velocimeter measurements in a centrifugal pump with a synchronously orbiting impeller, *J. Turbomachin.* **114**(2), 340–349 (1992)
- 14.100 R.C. Stauter: Measurement of the three-dimensional tip region flow field in an axial compressor, *J. Turbomachin.* **115**(3), 468–475 (1993)
- 14.101 M.D. Hathaway, R.M. Chriss, J.R. Wood, A.J. Strazisar: Experimental and computational investigation of the NASA low-speed centrifugal compressor flow field, *J. Turbomachin.* **115**(3), 527–542 (1993)
- 14.102 K.J. Farrell, M.L. Billet: A correlation of leakage vortex cavitation in axial flow pumps, *J. Fluids Eng.* **116**, 551–557 (1994)
- 14.103 M. Abramian, J.H.G. Howard: A rotating laser-doppler anemometry system for unsteady relative flow measurements in model centrifugal impellers, *J. Turbomachin.* **116**(2), 260–268 (1994)
- 14.104 J.R.J. Fagan, S. Fleeter: Comparison of optical measurement techniques for turbomachinery flow fields, *J. Propulsion Power* **10**(2), 176–182 (1994)
- 14.105 G.V. Hobson, B.E. Wakefield, W.B. Roberts: Turbulence amplification with incidence at the leading edge of a compressor cascade, *ASME* **96-GT-409** (1996)
- 14.106 M.A. Zaccaria, B. Lakshminarayana: Unsteady flow field due to nozzle wake interaction with the rotor in an axial flow turbine: Part 1 – rotor passage flow field, *J. Turbomachin.* **119**(2), 201–213 (1997)
- 14.107 D. Adler, R. Benyamin: Experimental investigation of the stator wake propagation inside the flow passages of an axial gas turbine rotor, *Int. J. Turbo Jet Engin.* **16**, 193–206 (1999)
- 14.108 D. Ristic, B. Lakshminarayana, S. Chu: Three-dimensional flow field downstream of an axial-flow turbine rotor, *J. Propulsion Power* **15**(2), 334–344 (1999)
- 14.109 M.B. Kang, K.A. Thole: Flowfield measurements in the endwall region of a stator vane, *J. Turbomachin.* **122**(3), 458–466 (2000)
- 14.110 T.M. Faure, G.J. Michon, H. Miton, N. Vassilieff: Laser Doppler anemometry measurements in an axial compressor stage, *J. Propulsion Power* **17**(3), 481–491 (2001)
- 14.111 D.E. Van Zante, W.-M. To, J.-P. Chen: Blade row interaction effects on the performance of a moderately loaded NASA transonic compressor stage, *Proc. of ASME Turbo Expo 2002* (ASME, Amsterdam 2002)
- 14.112 J. Woisetschlager, N. Mayrhofer, H. Lang, B. Hampel: Experimental investigation of turbine wake flow by interferometrically triggered PIV and LDV measurements, *Proc. ASME Turbo Expo 2002* (ASME, Amsterdam 2002)
- 14.113 X. Xiao, B. Lakshminarayana: Experimental investigation of end-wall flow in a turbine rotor, *J. Propulsion Power* **18**(5), 1122–1123 (2002)
- 14.114 T. Matsunuma, Y. Tsutsui: LDV measurements of unsteady mid-span flow in a turbine rotor at low reynolds number, *Proc. ASME Turbo Expo* (Atlanta, 2003)
- 14.115 S. Ibaraki, T. Matsuo, H. Kuma, K. Sumida, T. Suita: Aerodynamics of a transonic centrifugal compressor impeller, *J. Turbomachin.* **125**(2), 346–351 (2003)
- 14.116 T.M. Faure, H. Miton, N. Vassilieff: A laser Doppler anemometry technique for Reynolds stress measurement, *Exp. Fluids* **37**, 465–467 (2004)
- 14.117 L.E. Drain: *The laser Doppler technique* (Wiley, New York 1980)
- 14.118 H.B. Weyer: Optical methods of flow measurement and visualization in rotors, *Proc. Joint Fluids Engineering and Gas Turbine Conference* (New York 1980)
- 14.119 A. Doukelis, M. Founti, K. Mathioudakis, K. Pappiliou: Evaluation of beam refraction effects in a 3D laser Doppler anemometry system for turbo-



- machinery applications, *Measure. Sci. Technol.* **7**, 922–931 (1996)
- 14.120 W. Copenhaver, J. Esteveadoral, S. Gogineni, S. Gorrell, L. Goss: DPIV study of near-stall wake-rotor interactions in a transonic compressor, *Exp. Fluids* **33**(6), 899–908 (2002)
- 14.121 H. Lang, T. Morck, J. Woisetschlager: Stereoscopic particle image velocimetry in a transonic turbine stage, *Exp. Fluids* **32**(6), 700–709 (2002)
- 14.122 N. Balzani, F. Scarano, M.L. Riethmuller, F.A.E. Breugelmans: Experimental investigation of the blade-to-blade flow in a compressor rotor by digital particle image velocimetry, *J. Turbomachin.* **122**(4), 743–750 (2000)
- 14.123 M.P. Wernet, D.E. Van Zante, A.J. Strazisar, W.T. John, P.S. Prahst: 3-D digital PIV measurements of the tip clearance flow in an axial compressor, *Proc. ASME Turbo Expo* (Amsterdam, 2002)
- 14.124 O. Uzol, Y.-C. Chow, J. Katz, C. Meneveau: Unobstructed particle image velocimetry measurements within an axial turbo-pump using liquid and blades with matched refractive indices, *Exp. Fluids* **33**, 909–919 (2002)
- 14.125 R.J. Adrian: Multi-point optical measurements of simultaneous vectors in unsteady flow – a review, *Int. J. Heat Fluid Flow* **7**, 127–145 (1986)
- 14.126 C.E. Willert, M. Gharib: Digital particle image velocimetry, *Exp. Fluids* **10**(4), 181–193 (1991)
- 14.127 R.J. Adrian: Particle imaging techniques for experimental fluid mechanics, *Ann. Rev. Fluid Mech.* **23**, 261–304 (1991)
- 14.128 Westerweel: Fundamentals of digital particle image velocimetry, *Meas. Sci. Technol.* **8**, 1379–1392 (1997)
- 14.129 H. Huang, D. Dabiri, M. Gharib: On errors of digital particle image velocimetry, *Meas. Sci. Technol.* **8**, 1427–1440 (1997)
- 14.130 A. Melling: Tracer particles and seeding for particle image velocimetry, *Meas. Sci. Technol.* **8**, 1406–1416 (1997)
- 14.131 R.J. Adrian: Dynamic ranges of velocity and spatial resolution of particle image velocimetry, *Meas. Sci. Technol.* **8**, 1393–1398 (1997)
- 14.132 M. Raffel, C. Willert, J. Kompenhans: *Particle Image Velocimetry – A Practical Guide* (Springer, Berlin 1998)
- 14.133 R. Dong, S. Chu, J. Katz: Quantitative visualization of the flow within the volute of a centrifugal pump: Part A – Technique, *J. Fluids Eng.* **114**, 390–395 (1992)
- 14.134 D. Tisserant, F.A.E. Breugelmans: Rotor blade-to-blade measurements using particle image velocimetry, *J. Turbomachin.* **119**, 176–181 (1997)
- 14.135 J. Esteveadoral, S. Gogineni, W. Copenhaver, G. Bloch, M. Brendel: Flow field in a low-speed axial fan: A DPIV investigation, *Exp. Therm. Fluid Sci.* **23**, 11–21 (2000)
- 14.136 Y.-D. Choi, K. Nishino, J. Kurokawa, J. Matsui: PIV measurement of internal flow characteristics of very low specific speed semi-open impeller, *Exps. Fluids* **37**, 617–630 (2004)
- 14.137 J.M. Sankovic, J.R. Kadambi, M. Mehta, W.A. Smith, M.P. Wernet: PIV investigations of the flow field in the volute of a rotary blood pump, *J. Fluids Eng.* **126**, 730–734 (2004)
- 14.138 N. Paone, M.L. Riethmuller, R.A. Van den Braembussche: Experimental investigation of the flow in the vaneless diffuser of a centrifugal pump by particle image displacement velocimetry, *Exp. Fluids* **1989**, 371–378 (1989)
- 14.139 S. Chu, R. Dong, J. Katz: Relationship between unsteady flow, pressure fluctuations and noise in a centrifugal Pump – Part A: Use of PDV data to compute the pressure field, *ASME J. Fluids Eng.* **117**(1), 24–29 (1995)
- 14.140 S. Chu, R. Dong, J. Katz: Relationship between unsteady flow, pressure fluctuations and noise in a centrifugal pump – Part B: Effects of blade-tongue interactions, *ASME J. Fluids Eng.* **117**(1), 30–35 (1995)
- 14.141 K.M. Day, P. Lawless, S. Fleeter: Particle image velocimetry measurements in a low speed two stage research turbine, *AIAA 1996–2569*, 32nd ASME, SAE and ASEE Joint Propulsion Conference and Exhibit 1996, Lake Buena Vista (AIAA, Reston 1996)
- 14.142 R. Dong, S. Chu, J. Katz: Effect of modification to tongue and impeller geometry on unsteady flow, pressure fluctuations and noise in a centrifugal pump, *J. Turbomachin.* **119**(3), 506–515 (1997)
- 14.143 M. Sinha, J. Katz: Quantitative visualization of the flow in a centrifugal pump with diffuser vanes: Part 1 – on flow structures and turbulence, *J. Fluids Eng.* **122**, 97–107 (2000)
- 14.144 M.P. Wernet: A flow field investigation in the diffuser of a high-speed centrifugal compressor using digital particle image velocimetry, *Meas. Sci. Technol.* **11**, 1007–1022 (2000)
- 14.145 M.P. Wernet: Development of digital particle imaging velocimetry for use in turbomachinery, *Exp. Fluids* **28**(2), 97–115 (2000)
- 14.146 M.P. Wernet, M. Bright, G. Skoch: An investigation of surge in a high-speed centrifugal compressor using digital PIV, *J. Turbomachin.* **123**, 413–428 (2001)
- 14.147 O. Uzol, C. Camci: Aerodynamic loss characteristics of a turbine blade with trailing edge coolant ejection Part 2: external aerodynamics, total pressure losses and predictions, *J. Turbomachin.* **123**(2), 249–257 (2001)
- 14.148 M. Sinha, Pinarbasi., J. Katz: The flow structure during onset and developed states of rotating stall within a vane diffuser of a centrifugal pump, *J. Fluids Eng.* **123**, 490–499 (2001)
- 14.149 A.J. Sanders, J. Papalia, S. Fleeter: Multi-blade row interactions in a transonic axial compressor: Part 1

- stator particle image velocimetry (PIV) investigation, ASME J. Turbomachin. **124**(1), 10–18 (2002)
- 14.150 O. Uzol, Y.-C. Chow, J. Katz, C. Meneveau: Experimental investigation of unsteady flow field within a two stage axial turbomachine using particle image velocimetry, J. Turbomachin. **124**(4), 542–552 (2002)
- 14.151 Y.-C. Chow, O. Uzol, J. Katz: Flow non-uniformities and turbulent "hot spots" due to wake-blade and wake-wake interactions in a multistage turbomachine, ASME J. Turbomachin. **124**(4), 553–563 (2002)
- 14.152 J. Esteveordal, S. Gogineni, L. Goss, W. Copenhaver, S. Gorrell: Study of Wake-Blade Interactions in a Transonic Compressor Using Flow Visualization and DPIV, J. Fluids Eng. **124**, 166–175 (2002)
- 14.153 O. Uzol, Y.-C. Chow, J. Katz, C. Meneveau: Average passage flow field and deterministic stresses in the tip and hub regions of a multi-stage turbomachine, J. Turbomachin. **125**(4), 714–725 (2003)
- 14.154 Y.C. Chow, O. Uzol, J. Katz: *On the flow and turbulence within the wake and boundary layer of a rotor blade located downstream of an IGV, in ASME Turbo Expo 2003 International Gas Turbine Institute Conf. Atlanta* (ASME, Fairfield 2003)
- 14.155 J. Woisetschlager, N. Mayrhofer, B. Hampel, H. Lang, W. Sanz: Laser-optical investigation of turbine wake flow, Exp. Fluids **34**, 371–378 (2003)
- 14.156 O. Uzol, Y.C. Chow, F. Soranna, J. Katz: 3D structure of a rotor wake at mid-span and tip regions, Proc. of 34th AIAA Fluid Dynamics Conference and Exhibit (Portland, 2004)
- 14.157 O. Uzol, Y.-C. Chow, F. Soranna, J. Katz, C. Meneveau: 3D measurements of deterministic stresses within a rotor-stator gap at mid-span and tip regions, Proc. of ASME Heat Transfer/Fluids Engineering Summer Conference (Charlotte, 2004)
- 14.158 B.J. Liu, H.W. Wang, H.X. Liu, H.J. Yu, H.K. Jiang, M.Z. Chen: Experimental investigation of unsteady flow field in the tip region of an axial compressor rotor passage at near stall condition with stereoscopic particle image velocimetry, J. Turbomachin. **126**(3), 360–374 (2004)
- 14.159 F. Soranna, Y.-C. Chow, O. Uzol, J. Katz, C. Meneveau: Rotor boundary layer response to an impinging wake, ASME Heat Transfer/Fluids Engineering Summer Conference (Charlotte, 2004)
- 14.160 S.J. Lee, B.G. Paik, J.H. Yoon, C.M. Lee: Three-component velocity field measurements of propeller wake using a stereoscopic PIV technique, Exp. Fluids **34**, 575–585 (2004)
- 14.161 Y.C. Chow, O. Uzol, J. Katz, C. Meneveau: Decomposition of the spatially filtered and ensemble averaged kinetic energy, the associated fluxes and scaling trends in a rotor wake, Phys. Fluids **17**(8) (2005)
- 14.162 F. Soranna, Y.-C. Chow, O. Uzol, J. Katz: 3D Measurements of the Mean Velocity and Turbulence Structure within the Near Wake of a Rotor Blade, Proc. ASME Fluids Engineering Division Summer Meeting and Exhibition (Houston, 2005)
- 14.163 J. Esteveordal, T.R. Meyer, S.P. Gogineni: Development of a fiber optic PIV system for turbomachinery applications, AIAA, 0038 (2005)
- 14.164 U. Ullum, J.J. Schmidt, P.S. Larsen, D.R. McCluskey: Statistical analysis and accuracy of PIV data, J. Visualization **1**(2), 205–216 (1998)
- 14.165 O. Uzol, C. Camci: The effect of sample size turbulence intensity and velocity field on the experimental accuracy of ensemble averaged PIV measurements, Proc. 4th International Symposium on Particle Image Velocimetry (Göttingen, 2001)
- 14.166 J. J. Adamczyk: Model Equation for simulating flows in multistage turbomachinery, ASME Paper No. 85-GT-226 (1985)
- 14.167 J. J. Adamczyk, R. A. Mulac, M. L. Celestina: A model for closing the inviscid form of the average-passage equation system, ASME Paper No. 86-GT-227 (1986)
- 14.168 M. Sinha, J. Katz, C. Meneveau: Quantitative visualization of the flow in a centrifugal pump with diffuser vanes: Part 2 – addressing passage-averaged and LES modeling issues in turbomachinery flows, J. Fluids Eng. **122**, 108–116 (2000)
- 14.169 F. Soranna, Y.-C. Chow, O. Uzol, J. Katz: The effect of IGV wake impingement on the flow structure and turbulence around a rotor blade, J. Turbomachin. **128**(1), 82–95 (2006)
- 14.170 P.W. McDonald, C.R. Bolt, R.J. Dunker, H.B. Weyer: A comparison between measured and computed flow fields in a transonic compressor rotor, J. Eng. Power **102**, 883–891 (1980)
- 14.171 W.J. Calvert, A.W. Stapleton: Detailed flow measurements and predictions for a three-stage transonic fan, J. Turbomachin. **116**(2), 298–305 (1994)
- 14.172 X. Ottavy, I. Trebinjac, A. Vouillarmet: Analysis of interrow flow field within a transonic axial compressor: Part 1 – unsteady flow analysis, J. Turbomachin. **123**, 57–63 (2001)
- 14.173 C. Schodl, C. Willert, I. Roehle, J. Heinze, W. Foerster, M. Fischer, M. Beversdorff: Optical diagnostic techniques in turbomachinery, AIAA 2002-3038, 22nd AIAA Aerodynamic Measurement Technology and Ground Testing Conference (St. Louis, 2002)
- 14.174 K. Ziegler, E.H. Gallus, R. Niehuis: A study on impeller-diffuser interaction: Part 2 – detailed flow analysis, J. Turbomachin. **125**(1), 183–192 (2003)
- 14.175 K.R. Navarra, D.C. Rabe, S.D. Fonov, L.P. Goss, C. Hah: The application of pressure and temperature sensitive paints to an advanced compressor, J. Turbomachin. **123**(4), 823–829 (2001)
- 14.176 J.W. Gregory: Porous pressure sensitive paint for measurement of unsteady pressures in turbomachinery, Proc. 42nd Aerospace Sciences Meeting and Exhibit (ASME, Reno 2004)

- 14.177 Schodl R.: Development of the laser-two-focus method for non-intrusive measurement of flow vectors, particularly in turbomachines, European Space Agency Technical Translation ESA-TT-528 (1979)
- 14.178 Schodl R.: Laser-two-focus velocimetry. In: Advanced Instrumentation for Aero Engine Components. Papers Presented at the Propulsion and Energetics Panel 67th Symposium, AGARD Conference Proc., No. 399 (Philadelphia, 1986) p 7.1–7
- 14.179 X. Ottavy, I. Trebinjac, A. Vouillarmet: Treatment of L2F anemometer measurement volume distortions created by curved windows for turbomachinery applications, *Meas. Sci. Technol.* **9**, 1511–1521 (1998looseness1)
- 14.180 H. Komine: System for Measuring Velocity Field of Fluid Flow using a Laser Doppler Spectral Image Converter. US Patent No. 4919536 (1990)
- 14.181 H.D. Ford, R.P. Tatam: Development of extended field Doppler velocimetry for turbomachinery applications, *Opt. Lasers Eng.* **27**, 675–696 (1997looseness1)
- 14.182 I. Roehle, P. Voigt, C. Willert: Recent developments and applications of quantitative laser light sheet measuring techniques in turbomachinery components, *Meas. Sci. Technol.* **11**, 1023–1035 (2000)
- 14.183 M.P. Wernet: Planar particle imaging doppler velocimetry: a hybrid PIV/DGV technique for three-component velocity measurements, *Meas. Sci. Technol.* **15**, 2011–2028 (2004)
- 14.184 K. Sabroske, D. Rabe, C. Williams: Pressure-sensitive paint investigation for turbomachinery application, *ASME* **95-GT-92** (1995)
- 14.185 T. Liu, S. Torgerson, J. Sullivan, R. Johnston, S. Fleeter: Rotor blade pressure measurement in a high speed axial compressor using pressure and temperature sensitive paints, *Proc. 35th Aerospace Sciences Meeting Exhibit (ASME, Reno 1997)*
- 14.186 R.H. Engler, C. Klein, O. Trinks: Pressure sensitive paint systems for pressure distribution measurements in wind tunnels and turbomachines, *Meas. Sci. Technol.* **11**, 1077–1085 (2000)
- 14.187 J. Lepicovsky, T.J. Bencic: Use of pressure sensitive paint for diagnostics in turbomachinery flows with shocks, *Exp. Fluids* **33**, 531–538 (2002)
- 14.188 Bell, Schairer, Hand, Mehta: Surface pressure measurements using luminescent coatings, *Ann. Rev. Fluid Mech.* **33**, 155–206 (2001)